Routing Protocols for Ultra-Wideband Mobile Ad Hoc Networks

Der Fakultät für Elektrotechnik und Informatik
der Gottfried Wilhelm Leibniz Universität Hannover

zur Erlangung des akademischen Grades
Doktor-Ingenieur

genehmigte
Dissertation
von

M.Sc.-EE. Samer Bali
geboren am 03.Juni 1976 in Jericho

2008

1. Referent: Prof. Dr.-Ing. Klaus Jobmann

2. Referent: Prof. Dr.-Ing. Christian Grimm

Vorsitzender: Prof. Dr.-Ing. Jörn Ostermann

Tag der Promotion: 15.09.2008

ERKLÄRUNG

Hiermit erkläre ich, dass ich die vorliegende Dissertation selbstständig verfasst und keine anderen als die angegebenen Quellen und Hilfsmittel verwendet habe. Die vorliegende Dissertation wurde noch nicht als Diplom oder ähnliche Prüfungsarbeit verwendet.

Teile der Arbeit sind auf Fachkonferenzen veröffentlicht worden. Die Vorliegende Dissertation stellt mein erstes Promotionsgesuch dar.

Samer Bali

Hannover, den 02.07.2008.

ACKNOWLEDGEMENTS

ABSTRACT

Mobile Ad hoc Network (MANET) field is one of the most vibrant and active research fields in wireless communications networking. It can be considered as emerging fourth generation wireless system that connects devices anywhere and anytime. MANET can be built around any wireless technology. However, wireless communication networks have witnessed recently the introductory of a promising transmission technology called Ultra-Wideband (UWB). UWB technology has been investigated intensively in the last few years due to its many attractive properties (such as large channel capacity) and it is supposed to be a promising candidate for MANET in short range scenarios. One of the essential aspects of MANET is the development of routing protocols. In MANET, routing protocols are needed to establish and maintain connections between nodes.

The main goal of this thesis is to design efficient routing protocols for MANET based on UWB technology in a production line in a factory which is an industrial indoor application. However, UWB technology is still in the research and standardization phase during the time of performing this thesis. Therefore, the production line network scenario was defined and simulated in ns-2 simulator as basis for the investigations. In these investigations, Ad Hoc On-Demand Distance Vector (AODV), Dynamic Source Routing (DSR) and Optimized Link State Routing (OLSR) were considered in order to specify the basic requirements needed to design efficient routing protocols for the production line network scenario. Since the investigations are based on simulation results, closed-form formulas were found for the channel capacity of MANET as a tool for benchmarking and validation.

Based on the investigations, two approaches were proposed to design efficient routing protocols for the production line network scenario. The first approach is based on an enhanced routing protocol. In this protocol, some routing mechanisms of AODV, DSR and OLSR are combined in one efficient routing protocol. The second approach is based on a new routing protocol. Using this protocol in the production line network scenario, nodes can exploit the exchanged information between them to maintain and update routing tables without the use of extra routing control packets.

Based on the first approach, a new routing protocol suitable to the production line network scenario was designed and it was called Ad-Hoc On-Demand Multipath Source Routing (AOMSR) protocol. AOMSR was designed in a simple and robust way. It uses routing tables with multiple route paths per destination, time threshold to delete inactive routes, and destination sequence number to determine the freshness of a route. In addition, it uses source routing mechanism to determine free-loop and disjoint paths in a robust simple way. Furthermore, AOMSR makes use of disjoint paths to control number of forwarding nodes in the network and to establish reliable route paths. It was found that AOMSR outperforms the other routing protocols considered in this study.

Keywords: Routing Protocols, AODV, DSR, OLSR, MANET, UWB, Channel Capacity.

KURZFASSUNG

Mobile ad hoc Netze (Mobile Ad-Hoc Networks, MANETs) stellen eines der aktivsten Forschungsgebiete in der drahtlosen Vernetzung von Kommunikationssystemen dar. MANETs können als vierte Generation drahtloser Systeme aufgefasst werden, durch welche die Geräte überall und jederzeit drahtlos verbunden werden. MANETs können mit beliebigen drahtlosen Technologien realisiert werden. Mit Ultra-Breitband (Ultra-Wideband, UWB) steht drahtlosen Kommunikationsnetzen jedoch eine sehr vielversprechende neue Übertragungstechnologie zur Verfügung. UWB wurde in den letzten Jahren aufgrund vieler attraktiver Eigenschaften (z.B. hohen Kanalkapazität) intensiv für MANETs bei geringer Reichweite untersucht. Einer der wesentlichen Aspekte von MANETs ist die Entwicklung von Routing-Protokollen. In MANETs sind Routing-Protokolle erforderlich, welche zur Erstellung und Pflege von Verbindungen zwischen Knoten dienen.

Das Hauptziel dieser Arbeit ist die Erstellung von effizienten Routing-Protokollen für UWB-basierte MANETs in einer Fließbandfertigung einer Fabrik als Beispiel für eine typische, industrielle Anwendung. Momentan befindet sich die UWB-Technologie noch in einer Phase intensiver Forschungs- und Standardisierungsaktivitäten. Daher wurde das Netzwerkszenario Fließbandfertigung definiert und mit Hilfe des Simulationswerkzeugs NS-2 als Grundlage der Untersuchungen simuliert. In diesen Untersuchungen, wurden AODV (Ad Hoc On-Demand Distance Vector), DSR (Dynamic Source Routing) und OLSR (Optimized Link State Routing) betrachtet, um die grundlegenden Anforderungen für die Erstellung von effizienten Routing-Protokollen für das Netzwerkszenario festzulegen. Weil die Untersuchungen auf Simulationsergebnissen basieren, wurden außerdem geschlossene mathematische Formeln für die Kanalkapazität von MANETs hergeleitet und als Instrument für die Validierung der Simulationsergebnisse verwendet.

Basierend auf den Untersuchungen wurden anschließende zwei Ansätze vorgeschlagen, um effiziente Routing-Protokolle für das Netzwerkszenario zu erstellen. Der erste Ansatz basiert auf einem verbesserten Routing-Protokoll. In diesem Protokoll wurden einige Routing-Mechanismen des AODV, DSR und OLSR zu einem effizienten neuen Routing-Protokoll kombiniert. Der zweite Ansatz basiert auf einem neuartigen Routing-Protokoll. Mit diesem Protokoll können Knoten die zwischen ihnen ausgetauschten Informationen direkt nutzen, um Routing-Tabellen zu pflegen und zu aktualisieren ohne zusätzliche Routing-Kontrollepakete zu verwenden. Basierend auf dem ersten Ansatz wurde ein neues Routing-Protokoll mit dem Namen AOMSR (Ad-Hoc On-Demand Multipath Source Routing) spezifisch für das Netzwerkszenario erstellt. AOMSR wurde als einfaches und robustes Protokoll konzipiert.

Es verwendet Routing-Tabellen mit mehreren Routing-Pfaden pro Ziel, Zeit-Schwellen, um inaktive Routen zu löschen sowie Ziel-Sequenznummern, um die Frische der Route zu bestimmen. Zusätzlich nutzt das Protokoll den Quell-Routing-Mechanismus, um Frei-Schleifen und disjunkte Wege einfach festzustellen. Außerdem nutzt AOMSR disjunkte Wege, um die Anzahl der Weiterleitungsknoten im Netz zu kontrollieren und sichere Routing-Pfade zu etablieren. Es konnte nachgewiesen werden, dass AOMSR die anderen betrachteten Routing-Protokolle übertrifft.

Stichworte: Routing-Protokolle, AODV, DSR, OLSR, MANET, UWB, Kanalkapazität.

TABLE OF CONTENTS

LIST OF FIGURES AND TABLES

Figures

Tables

LIST OF ACRONYMS

AODV   Ad hoc On-demand Distance Vector

AOMDV   Ad Hoc On-Demand Multipath Distance Vector

AOMSR   Ad hoc On-demand Multipath Source Routing

CD   Compact Disk

CSMA   Carrier Sense Multiple Access

CSMA/CA   Carrier Sense Multiple Access with Collision Avoidance

DSR   Dynamic Source Routing

DYMO   Dynamic MANET On-demand

ETSI   European Technical Standards Institute

FCC   Federal Communications Commission

G4   fourth Generation

ID   Identity

IKT   Institute for Communications Technology

IR-UWB   Impulse Radio Ultra-Wideband

LOS   Line of Sight

MAC   Medium Access Control

MANET   Mobile Ad hoc Network

MC-UWB   Multi-Carrier Ultra-Wideband

MPR   Multipoint Relay

NLOS   Non Line of Sight

NS-2   Network Simulator 2

NTh   Normalized Throughput

OLSR   Optimized Link State Routing

OLSRv2   Optimized Link State Routing Protocol version 2

OTcl   Object Tool Command Language

PDR   Packet Delivery Ratio

PHY   Physical

PPM   Pulse Position Modulation

PR   Pseudo Random

PULSERS   Pervasive Ultra-wideband Low Spectral Energy Radio Systems

RERR   Route Error

ROR   Routing Overhead Ratio

RREP   Route Reply

RREQ   Route Request

TC   Topology Control

TCP	Transmission Control Protocol
TH	Time Hopping
TH-IR-UWB	Time Hopping Impulse Radio Ultra-Wideband
UCAN	Ultra wideband Concepts for Ad-hoc Networks
UFZ	UWB Friendly Zone
UWB	Ultra-Wideband
WLAN	Wireless Local Area Network
WPAN	Wireless Personal Area Network

1 INTRODUCTION

Mobile Ad hoc Network (MANET) field is one of the most vibrant and active research fields in wireless communications networking. MANET can be considered as emerging fourth generation (G4) wireless system that connects devices anywhere and anytime. There are vast variety of MANET applications that have drawn great attention in many fields such as military, emergency services, sensor networks, industry, business, education and entertainment. In this thesis, we have considered an industrial indoor application in a factory.

A MANET is formed by self-configurable mobile devices that have wireless capabilities in order to establish multi-hop communications among them. Figure 1.1 shows an example of a simple MANET in a factory. In such networks, nodes are connected via wireless links that are established and disposed spontaneously without relying on a pre-existing infrastructure. In general, a MANET has a dynamic topology in which nodes may enter and exit the network at any time due to many reasons such as node mobility, battery capacity and link failures.

Figure 1.1: Example of a Simple MANET.

One of the essential aspects of MANET is the development of routing protocols. In MANET, routing protocols are needed to establish and maintain connections between nodes. All nodes in MANET may operate as routers and they cooperate to forward data packets to each other. Therefore, a great number of routing protocols have been proposed for MANET in literature. There is not a clear dominance of one protocol over the other, i.e., some routing protocols are likely to perform best in one network scenario, while others perform better in a different network scenario. However, MANET working group [32] is trying to standardize two routing protocols based on Ad Hoc On-Demand Distance Vector (AODV), Dynamic Source Routing (DSR) and Optimized Link State Routing (OLSR) because these three routing protocols achieve the best performance in most network scenarios. Therefore, we focused in our investigations on these three routing protocols to develop appropriate routing protocol(s) that can be used in our factory scenario.

MANET can be built around any wireless technology. Recently, wireless communication networks have witnessed the introductory of a promising transmission technology called Ultra-Wideband (UWB). UWB technology has been investigated intensively in the last few

years due to its many attractive properties such as high data rates, very low transmission power, spectrum reuse, robust performance under multi-path conditions, multiple access capabilities and high resolution position location and tracking. UWB transmission technique is supposed to be a promising candidate for MANETs in short range scenarios.

The main goal of this thesis is to establish efficient routing protocols for MANET based on UWB technology in an industrial indoor application. To achieve this goal, simulation software has been developed as basis for investigations. In this software, two basic considerations have been taken into account. Firstly, we have considered a physical layer model that uses an UWB transmission technique. Secondly, we have considered a realistic network scenario that represents an industrial indoor application in a factory. In this scenario, we have considered realistic mobility and traffic patterns as well. A secondary goal of this thesis is to develop a mathematical a model for the channel capacity of MANET based on UWB technology as a tool for benchmarking. Another goal of this thesis is to justify the use of UWB technology in MANET in indoor applications by comparing its performance and capabilities with that of WLAN technology.

To achieve these goals, the following methodology is used:

- define and simulate a network scenario as basis for investigations, considering:
  - realistic radio propagation model,
  - realistic node positions and traffic patterns,
- carry out performance evaluation of routing protocols in order to specify the basic requirements needed to design a suitable routing protocol for our network scenario,
- develop a mathematical model for channel capacity as a tool for benchmarking and validation of simulation results,
- design efficient routing protocols for our network scenario.

Two publications and one award have been achieved based on this thesis. The first publication is a conference paper [6] that presents our simulation investigations. The second publication is also a conference paper [5] that describes our mathematical model for the channel capacity. Also, this thesis was awarded the second place prize for the best PhD student paper and poster [4] accepted and presented in IEEE Sarnoff Symposium held in Princeton, USA, on April 30, 2008.

1.1   Research Questions

This research answers the following questions:

- Which network scenario can make use of UWB technology, and why?
- Which routing protocol is best for this network scenario?
- How does a routing protocol affect the network performance?
- Which tools should be used?

UWB technology is suitable for MANET in indoor applications as we will see in the next chapter. A production line in a factory is a viable industrial indoor application. In this application, UWB technology can be applied because of its robust performance under multipath conditions, low transmission power and large channel capacity.

Investigations are needed to propose a suitable routing protocol for our network scenario. In general, a MANET routing protocol consists of two main mechanisms: route discovery and route maintenance. The differences in routing mechanisms will lead to different performance results. Therefore, we have chosen to develop one or both mechanisms to cope with the requirements of our network scenario.

UWB technology is still in the research and standardization phase during the time of performing this thesis. Therefore, we have simulated our network scenario in a well known network simulator as basis for investigations. Channel capacity is an important parameter in the evaluation and design of MANETs. Since our investigations are based on simulation results, we have developed a mathematical model for the channel capacity of MANET as a tool for benchmarking and validation.

1.2 Related Work

Many studies of MANET routing protocols have been carried out in the last decade. Most of these studies assume a primitive Physical (PHY) layer model and a random way point scenario, e.g., [10] and [17]. Very few studies consider a realistic scenario with a very simple realistic PHY layer model, such as [28]. However, our study differs from the previous ones substantially. Firstly, we have considered a PHY layer model that uses UWB transmission technique. Secondly, we considered a network scenario that represents an industrial indoor application.

In the last few years there has been a great interest in computing the channel capacity of ad hoc networks using analytical calculations. For example, in [23] the authors found asymptotic values for the throughput capacity per node in ad hoc networks in which the nodes are uniformly distributed on a unit desk. With similar network topology, the authors of [44] found also asymptotic values for the throughput capacity per node but they considered a different communication model in which each node has a limited transmission power and uses a huge bandwidth such as in UWB communications. In [25] the authors propose a new model to find a closed-form formula for interference level and channel capacity in ad hoc networks with honey-grid configuration based on Wireless Local Area Network (WLAN) technology. In contrast to [23] and [44], a closed-form formula for channel capacity of ad hoc networks with line topology is found in this thesis using a systematic model based on the model proposed in [25]. With this model, the effects of spread-spectrum techniques and medium access schemes on channel capacity can be easily determined.

1.3 Thesis Organization

This thesis is organized as follows:

Chapter 2 gives an overview on UWB. In this chapter, we present some UWB aspects and techniques that are relevant to this thesis. We also explain why UWB technology is suitable for MANET in indoor applications.

Chapter 3 gives an overview on possible MANET routing protocols that may be used in UWB networks.

Chapter 4 presents and discusses our experimental results. In this chapter, we define and describe our simulated network scenario and present a performance evaluation of AODV, DSR and OLSR in order to specify the basic requirements needed to design a suitable routing protocol for our network scenario.

Chapter 5 presents the developed mathematical model for the channel capacity of our network scenario. This model will be used as a tool for benchmarking and validation in order to justify the experimental results.

Chapter 6 describes in details our approach to design an enhanced routing protocol suitable for our network scenario. Then the performance of the new routing protocol is presented and compared to the performance of AODV, DSR and OLSR.

Finally, Chapter 7 summarizes and concludes this thesis. Also, an outlook for future work based on this thesis is presented.

2 ULTRA-WIDEBAND COMMUNICATIONS

Wireless communication networks have recently witnessed the introductory of a promising transmission technology called Ultra-Wideband (UWB). UWB system is defined as a radio system that has a 10-dB bandwidth that is either larger than 20% of its center frequency, or occupies 500 MHz or more [19]. The fractional bandwidth is defined [19] as the ratio of the energy bandwidth to the center frequency and it is given by

$$\text{Fractional Bandwidth} = \frac{2(f_H - f_L)}{(f_H + f_L)} \tag{2.1}$$

where f_H and f_L are the higher and lower -10dB frequencies respectively that determine the signal bandwidth as shown in Figure 2.1.
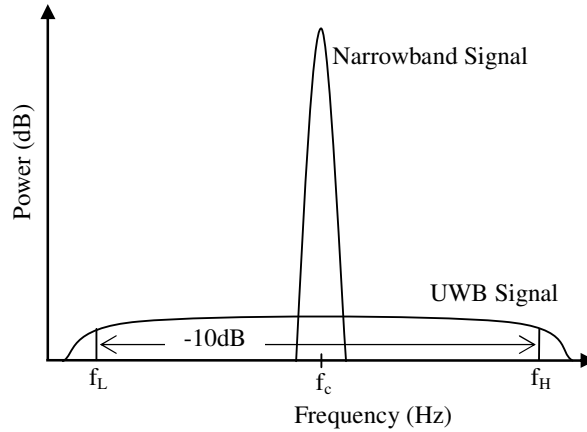
Figure 2.1: Comparison between Narrowband Signal and UWB Signal Bandwidths.

UWB technique has been investigated intensively in the last few years due to its many attractive properties that make it suitable for wireless communications in short range scenarios. The Preliminary results show that UWB has many benefits and characteristics including high data rates, large channel capacity, very low transmission power, spectrum reuse, robust performance under multi-path conditions, multiple access capabilities, and high resolution position location and tracking.

A bandwidth of 7.5GHz at -41.3dB/MHz is allocated for UWB communication systems [19]. If the entire bandwidth is fully utilized, the transmission power will be approximately 1mW. This is a much lower power of what is available to other communication systems such as WLAN operating with IEEE 802.11a/b/g standards. This makes UWB transmission technique a suitable candidate for the Physical Layer (PHY) of MANETs for low power, short range indoor applications. Therefore, IEEE 802.15.4a [26] subgroup was established to design and standardize UWB PHY layer for Wireless Personal Area Networks (WPAN).

In the next sections, we give a brief description of UWB history and radio regulation. Also, we present some aspects of UWB technology that are relevant to this thesis.

2.1 Brief History of UWB

The new history of UWB goes back to the early 1960s from work in time-domain electromagnetic when engineers from many laboratories and universities performed some of the original research on pulse transmitters, receivers and antennas [8], [7]. A major milestone in the development of UWB communication occurred when the sampling oscilloscope was developed in the 1960s. This oscilloscope did not only display and integrate UWB signals, but also provided simple circuits necessary for sub-nanosecond base-band pulse generation [8], [20].

As electronic component technology evolved in the early of 1970s, the basic designs for UWB communication and radar systems evolved as well. For example, the invention of sensitive base-band pulse receiver in 1972, led to the first patented design of a UWB communications system by Ross at Sperry Rand Corporation [52]. The first ground penetrating radar based on UWB was commercialized in 1974 by Morey at the Geophysical Survey Systems Corporation.

With the continuing development of UWB systems, many regulatory bodies, such as Federal Communications Commission (FCC) in the United States (and later the UWB Friendly Zone (UFZ) in Singapore and the European Technical Standards Institute (ETSI) in the European Union, took the task to authorize the use of UWB systems. This initiated a great amount of interest and fear towards UWB technology. As a result of the ambiguity of how UWB systems could operate with other existed systems, many UWB interference studies were performed in the late 1980s and in the 1990s. For example, Robert Scholtz at the University of Southern California wrote a land-mark paper that presented a multiple access technique for UWB communication systems [53]. As more studies concluded that UWB will be a possible candidate for wireless communications, investigations into UWB propagation and channel models were carried out in the late 1990s and early 2000s, e.g., see [11], [15], [16], [22], [40] and [54].

Recently there have been a very increasing number of companies and government agencies worldwide that are concerned about UWB technology. To be precise, interest in UWB has been sparked when the FCC issued a Report and Order in April 2002 allowing its commercial deployment with a given spectral mask requirement for both indoor and outdoor applications [19]. In 2003, the first FCC certified commercial system was installed [42], and in April 2003 the first FCC-compliant commercial UWB chipsets were announced by Time Domain Corporation. Also the European Union has funded many projects that are involved with UWB such as UCAN [61] and PULSERS [51] projects.

2.2 UWB Radio Regulations

In September 1998, the FCC issued a Notice of Inquiry related to the revision of Part 15 rules to allow the unlicensed use of UWB devices. Research in communications and radio technology showed that sharing the radio frequency spectrum among many users or services is more efficient than assigning fixed narrowband channels for each one. Therefore, instead of dividing the spectrum into distinct bands that were then allocated to specific users, FCC allowed UWB devices to operate with other existing services at a low enough power level that would not degrade the performance of these services.

By May 2000, the FCC had received more than 1000 documents from more than 150 different organizations in response to their Notice of Inquiry, to help the FCC in developing an appropriate set of specifications. In April 2002, the FCC issued a First Report and Order [19], which classified UWB operation into three separate categories:

- Communication and Measurement Systems,
- Vehicular Radar Systems,
- Imaging Systems, including Ground Penetrating Radar, Through-Wall Imaging and Surveillance Systems and Medical Imaging.

Each category was allocated a specific spectral mask. For example, Figure 2.2 shows the emission limits for UWB communication systems.
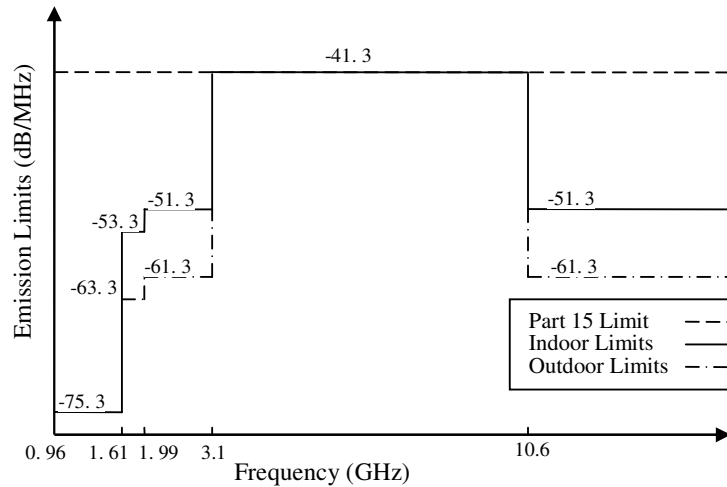
Figure 2.2: FCC Emission Mask for UWB Communication Systems.

Outside the United States, a similar approach has been used by many countries on the way to license UWB technology. In both Europe and Asia, initial studies have been accomplished and regulations have been issued by many regulatory bodies such as UFZ in Singapore and ETSI in the European Union. More information on the standards of UFZ and ETSI can be found in [57].

2.3   Impulse Radio UWB

There are mainly two forms of UWB: Impulse Radio UWB (IR-UWB) and Multi-Carrier UWB (MC-UWB). IR-UWB is based on sending very short duration pulses to transmit data, while MC-UWB using multiple simultaneous carriers. IR-UWB is recommended by IEEE 802.15.4a [26] subgroup to be used in indoor applications. Therefore, the focus will be on IR-UWB approach and other related schemes used in this thesis.

2.3.1   IR-UWB Signal

IR-UWB does not use a modulated sinusoidal carrier to transmit data as in the traditional narrowband signals. Instead, it uses a series of base-band pulses. The duration of these pulses are extremely short (in nanosecond order or shorter), therefore the power of transmitted pulse is spread over a wide range of frequencies as shown in Figure 2.1. In IR-UWB, the

unmodulated transmitted pulse can be represented by the second derivative of the Gaussian pulse [3] given by the following equation:

$$s(t) = A \cdot \left(1 - 4\pi \left(\frac{t}{\tau}\right)^2\right) \cdot e^{-2\pi \left(\frac{t}{\tau}\right)^2}$$

(2.2)

where A is the pulse amplitude and τ is used to adjust the pulse duration T_p. The second derivative of the Gaussian pulse represented by (2.2) is plotted in Figure 2.3 where A is 1 and τ is 1ns.
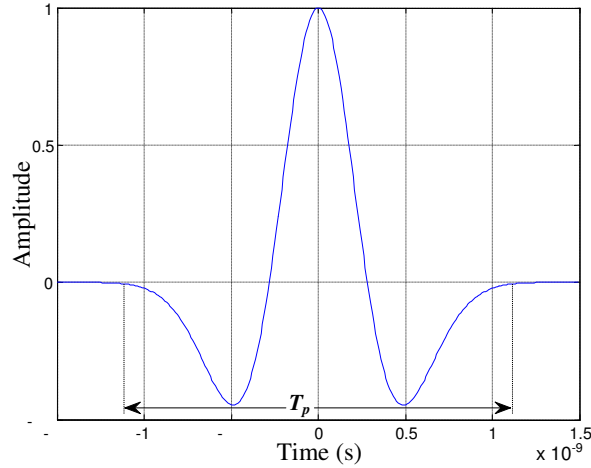
Figure 2.3: The second derivative of the Gaussian pulse.

2.3.2   Pulse Position Modulation

Many modulation schemes can be used with IR-UWB. Pulse Position Modulation (PPM) is used here as an example. With PPM, each bit is represented by a certain shift in the position of the UWB pulse. In a binary system for example, the bit 0 is represented by a pulse originating at the time instant 0, while the bit 1 is shifted in time by the amount of δ from time instant 0. Mathematically, the IR-UWB pulse given in (2.2) with PPM can be represented by:

$$x_j(t) = s(t - \delta \cdot d_j)$$

(2.3)

where d_j, assuming a binary system, is defined as following:

$$d_j = \begin{cases} 0, & j = 0 \\ 1, & j = 1 \end{cases}$$

(2.4)

2.3.3   Time Hopping IR-UWB

Time Hopping (TH) is the multiple access technique used in this thesis. Using TH maximizes channel utilization because all users (or nodes) can access the channel simultaneously using

8

Pseudo Random (PR) codes. Figure 2.4 shows the construction of one bit in TH-IR-UWB system. Here, one data bit time T_s consists of N_s TH frames with time duration T_f. Each TH frame consists of M_f chips with duration T_c. Therefore, one data bit is represented by N_s pulses. Each TH frame should contain only one pulse and the PR code determines the chip in which the pulse should occur. Pulse position in the chip is determined by the bit used to modulate the pulse.
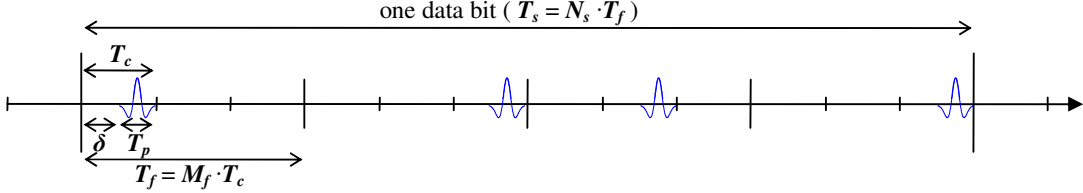
Figure 2.4: TH-IR-UWB System Concept.

The values of N_s and M_f typically range from a hundred to a thousand. In Figure 2.4, N_s is 4 and M_f is 3 for illustration reasons only. The transmission bit rate or symbol rate R_s can be defined in terms of frames time used to represent one data bit as following:

$$R_s = \frac{1}{T_s} = \frac{1}{N_s \cdot T_f}$$ (2.5)

A typical representation of the information signal for the mth user using TH-IR-UWB with PPM is given by:

$$x^{(m)}(t) = \sum_{k=-\infty}^{\infty} \sum_{j=0}^{N_s-1} s\left(t - k \cdot T_s - j \cdot T_f - c_j^{(m)} \cdot T_c - d_j^m \cdot \delta\right)$$ (2.6)

2.3.4 Processing Gain

As mentioned in the previous subsection, one data bit in TH-IR-UWB system is represented by N_s pulses. This technique is used to achieve processing gain that can combat noise and interference. This is similar to the approach used in spread spectrum systems. Therefore, the processing gain in dB based on this technique is given by [47]:

$$PG_1 = 10 \log_{10}(N_s)$$ (2.7)

Unlike spread spectrum systems, IR-UWB pulse does not occupy the entire frame time. Therefore, the duty cycle is extremely low since the pulse duration is very small compared to the frame time. Consequently, the impact of noise and interference is reduced so that it is only relevant when the pulse is being detected. This leads to processing gain in the sense of a spread spectrum system's ability to reduce the impact of noise and interference. Processing gain due to the low duty cycle is given by [47]:

$$PG_2 = 10\,log_{10}\left(\frac{T_f}{T_p}\right) \tag{2.8}$$

Total processing gain g is the sum of these two processing gains [60]. That is, g in dB is given by:

$$g = PG_1 + PG_2 \tag{2.9}$$

where PG_1 and PG_2 are given in equations (2.7) and (2.8) respectively. Therefore, UWB technology has a very large processing gain when compared to the traditional spread spectrum systems such as WLAN. As we will see in Chapter 5, large processing gain leads to large channel capacity as well. This is one more reason to make UWB transmission technique a suitable candidate for PHY layer of MANETs for low power, short range indoor applications with a noisy environment. Large channel capacity provides us with larger space in designing efficient routing protocols for our network scenario as we will see in Chapters 3 and 6.

2.4   UWB Pathloss Model

In indoor applications with a noisy and fading environment, the received power at certain distance from the transmitter can be described as a random variable due to multipath propagation effects, which are also known as fading effects. In this thesis, the shadowing model described in [21] is used to reflect UWB pathloss model in the PHY layer. In this model, the pathloss in dB at a certain distance d is given by:

$$PL(d) = \left(PL_o + 10\beta\,log_{10}\left(\frac{d}{d_o}\right) + S(d)\right), \qquad d \geq d_o \tag{2.10}$$

where PL_o is the pathloss at the intercept point d_o which is usually equals to 1m, β is the pathloss exponent and $S(d)$ is the log-normal shadow fading that reflects the variation of the received power at certain distance. $S(d)$ is considered to be a Gaussian random variable with zero mean and standard deviation σ_s. The values of PL_o, β and σ_s are determined depending on the network scenario. By using the shadowing model, the coverage area of a node cannot be represented by a circle because $S(d)$ is a random variable.

2.5   Summary and Conclusions

In this chapter, a brief description of UWB history and radio regulation is given. Also, IR-UWB signal, PPM, TH-IR-UWB technique, processing gain and UWB pathloss model are presented. These are some aspects of UWB technology that are implemented in the simulation software used in this thesis. IR-UWB is based on sending very short duration pulse that can be represented by the second derivative of the Gaussian pulse. PPM and TH techniques can be used with IR-UWB to construct a multiple access communication system. TH-IR-UWB system has a large processing gain that comes from the frame repetition and the low duty

cycle of the pulse. The shadowing model can be used to reflect UWB pathloss model in the PHY layer for indoor applications with a noisy and fading environment.

In this thesis, we have defined a network scenario as basis for our investigations of routing protocols. The network scenario represents an industrial indoor application that uses UWB technology. A viable industrial indoor application is a production line in a factory. UWB technology is suitable for indoor applications with a noisy environment because of its robust performance under multipath (or fading) conditions and low transmission power. Moreover, UWB technology has a very large processing gain when compared to the traditional spread spectrum systems such as WLAN. Large processing gain accompanied with large channel capacity makes UWB technology a good choice for industrial indoor applications.

In the next Chapter, we give an overview about possible MANET routing protocols that may be used in UWB networks.

3 MANET ROUTING PROTOCOLS

The development of routing protocols is one of the vital research fields in MANET. Therefore, there exists a vast variety of routing protocols designed for MANET in the literature. Any of these routing protocols can be used in UWB MANET. Routing protocols in MANET can be categorized based on several approaches. The most popular ones are based on proactive, reactive or hybrid approaches. Other classifications such as topology-based and position-based approaches are also used. In this thesis we focused on proactive and reactive routing protocols since MANET working group [32] is aiming to design two routing protocols based on these two approaches.

Proactive routing protocols, also called table-driven protocols, have been developed from the traditional distance vector [31] and link state [41] protocols designed for wired networks. In proactive approaches, each node in the network retains a route to all other nodes in all times. Route creation and maintenance are accomplished by a combination of periodic and event-triggered routing updates. Periodic updates occur between nodes at a specific time intervals regardless of any other factor. On the other hand, event-triggered updates take place whenever there is a change in the mobility or traffic characteristics of the network. Proactive approaches have the advantage that routes are immediately available whenever they are requested. However, the main disadvantage of these approaches is the addition of significant control overhead in large networks or in networks with rapidly moving nodes.

Reactive routing protocols, also called on-demand protocols, have been proposed as a new solution for routing in MANET. They are not derived from any pre-existing protocol but designed to meet the specific requirements of ad hoc networks. In reactive approaches, a route to a destination node is only discovered whenever it is actually needed. When a source node needs to send data packet to a certain destination node, it checks its route table to determine whether it has a route. If no route exists, a route discovery procedure is initiated to find a route to the destination node. Hence, route discovery is initiated on-demand only. When a route is discovered, it remains valid for a certain time and then it is discarded. The benefit of reactive approaches is the reduction of the control overhead, particularly in networks with low to moderate traffic loads. However, the primary drawback of these approaches is the introduction of a high initial latency in packet delivery.

MANET [32] is trying to standardize two routing protocols: Dynamic MANET On-demand (DYMO) Routing [12] as a reactive protocol and the Optimized Link State Routing Protocol version 2 (OLSRv2) [13] as a proactive protocol. However, we did not use these two routing protocols in our study since they are immature in terms of implementations. Moreover, they are basically developed from AODV, DSR and OLSR, and they differ mainly in packet header format. Therefore, we focused on AODV, DSR and OLSR in our study because they represent the current design choices of routing protocols considered by MANET. Furthermore, AODV, DSR and OLSR represent very different design choices and vary in how dynamic they are. In the following subsections, we describe AODV, DSR and OLSR protocols and summarize their respective advantages and disadvantages.

3.1 Ad Hoc On-Demand Distance Vector

AODV [48] represents an interesting attempt to exploit the advantages of the distance vector algorithms while maintaining a pure reactive approach by which each node maintains a routing table for active destinations only. In AODV, sequence numbers are used to avoid looping problems. When a source node wants to send a packet to a destination, it first checks its route table to determine if it has already a valid route to the destination. If a valid route does not exist, then it initiates a route discovery process by flooding a Route Request (RREQ) packet through the network. RREQ does not contain a complete path with all addresses of involved nodes. It contains the address and the last known sequence number for the destination node, the address and current sequence number of the source node, hop count initialized to zero, and RREQ Identity (ID). The RREQ ID is a per-node, monotonically increasing counter that is incremented each time the node initiates a new RREQ. In this way, the source address together with the RREQ ID uniquely identifies a RREQ and can be used to detect duplicates. When a RREQ is sent, it is flooded until it reaches the destination node or an intermediate node with a valid route to the destination. Flooding in AODV is a process by which a message can reach every node in the network. The first time a node receives the message, it forwards it to all its neighbors, and so on until every node has received at least one copy of the message. The principle is illustrated in Figure 3.1(a).

(a) RREQ Propagation   (b) RREP Propagation   (c) RERR Propagation
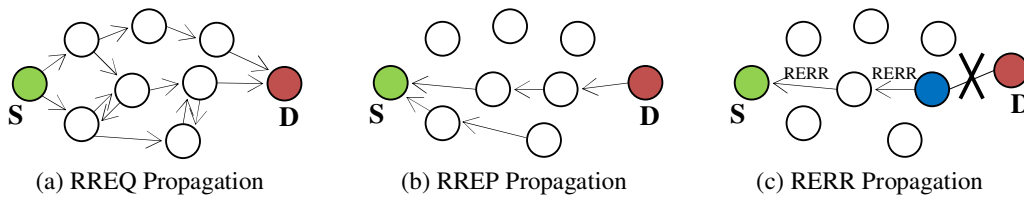
Figure 3.1: AODV Route Mechanisms.

A node can reply to a RREQ only if it has a corresponding sequence number greater or equal to that contained in the RREQ. This will ensure that the most recent route is selected, and also guarantees loop freedom. During the flooding process, nodes that forward a RREQ keep the address of the neighbor from which they received the first copy of the packet. Once the RREQ has reached the destination or an intermediate node with a valid route, a Route Reply (RREP) packet is sent back to the source via a unique path because nodes along the route forward it only to the node from which they received the RREQ. These nodes record the address of the neighbor which sent them the RREP in their routing table. If the source receives more than one RREP, it selects the route with the greatest sequence number and smallest hop count. Thus, AODV stores only one route per destination in its route table with a certain lifetime. An example of RREP propagation is illustrated in Figure 3.1(b).

Once a route is established, it must be maintained as long as it is needed. Because of the mobility of nodes, links along paths are likely to break. Breaks on links that are not being used for a certain threshold time do not require any repair. However, breaks in active routes must be quickly repaired so that data packets are not dropped. This is done by the use of Route Error (RERR) packet. When a node detects a failure on one of its outgoing links, it creates RERR packet which contains a list of all the destinations that are now unreachable due to the loss of the link. Then the node sends this RERR to its upstream neighbors that were

also using the lost link. Thus the RERR traverses the reverse path to the source node, as illustrated in Figure 3.1(c), causing the activation of new path discovery procedure if the route is still needed.

AODV principle is quite simple and it could be more efficient than proactive protocol in large networks with low traffic. Moreover, its routing overhead is relatively small compared with routing overhead produced using a proactive approach. The major drawback of this protocol is that it only supports symmetrical links. It cannot work if there is an asymmetrical link on the way back from destination (in such a case the RREP gets lost). Another negative point of this protocol is the delay in establishing a route in comparison with proactive protocols and protocols that support multipath routing. This delay could be a limiting factor in networks with high traffic or quick moving nodes because it will reduce network throughput.

3.2 Dynamic Source Routing

DSR [27] is similar to AODV in that it is a reactive routing protocol but it has a few important differences. One of the primary characteristics of DSR is that it is a source routing protocol, i.e., instead of being forwarded hop by hop, data packets contain strict source routes that specify each node along the path to the destination.
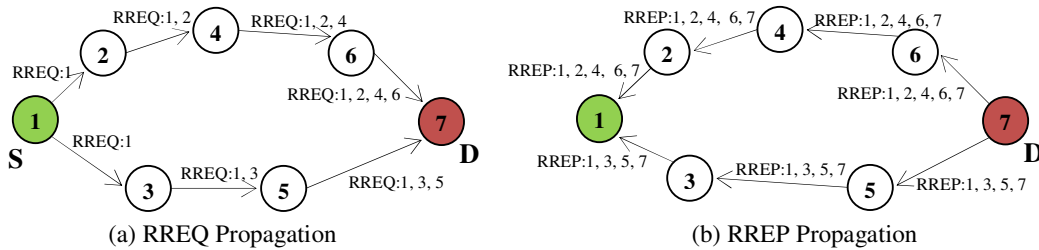
Figure 3.2: DSR Route Mechanisms.

In DSR, when a source node wants to send a data packet, it checks first its route cache for a route to the destination node. If this route is not available, a route discovery procedure is initiated, by which a RREQ is transmitted to all neighbors through the network until it reaches the destination node. RREQ contains address of the source node, address of destination and RREQ ID number. When an intermediate node forwards RREQ, it adds its own address to the route record of the packet. It forwards it only the first time it receives it and if its own address does not already appear in the route record (to avoid loops). Therefore, when RREQ arrives to destination it contains a complete path from source to destination, as shown in Figure 3.2(a).

When the packet reaches the destination or a node with a valid route to the destination, a RREP is generated. If the node knows a valid route to the source it can use it to send RREP. Otherwise, it can either use the reverse path in the route record of the route discovery packet (if symmetrical links are supported only), or it initiates its own path discovery including the route record in the packet (if symmetrical links cannot be assumed). RREP propagation is illustrated in Figure 3.2(b).

If a RREP packet is received, a route maintenance procedure is activated, which will maintain the route active until it is necessary. Route maintenance is accomplished through the use of

acknowledgements and RERR messages. Acknowledgements are used to verify the correct operation of the links in a path from source to destination. If a node is unable to reach a next-hop node after a certain number of retransmissions, a RERR message is sent to the original sender of the data packet to report a link failure.

Other characteristics that distinguish DSR from other reactive routing protocols include the fact that DSR uses route cache which allows multiple route entries to be maintained per destination, and therefore enabling multipath routing. When a link breaks, the source can use alternate routes from the route cache to prevent another route discovery. Also, DSR's route cache entries have not lifetimes. Once a route is placed in the route cache, it remains there until it breaks. The main disadvantage of this protocol is that it introduces large amount of routing overhead and does not scale well for use in large networks, since all routing information has to be carried in packet headers. Another drawback of DSR is that route entries do not have lifetimes, and this exposes DSR to stale routes.

3.3   Optimized Link State Routing

Unlike AODV and DSR, OLSR [14] is a proactive link state routing protocol. It is mainly optimized by three mechanisms: neighbor sensing, Multipoint Relays (MPRs) and Topology Control (TC) messages. Two nodes are considered as one-hop neighbors if there exists a link between them, and this link can be symmetrical or not. Two nodes are two-hop neighbors if they have a common neighbor to which they are related via symmetrical links. Each node periodically emits "hello" messages containing its own address, the addresses of all its known neighbors and the state of the link with them (unidirectional or bidirectional). By this mean every node can maintain information about its one-hop neighborhood and two-hop neighborhood. Such information remains valid for a limited period of time and must be refreshed at regular intervals.

In OLSR, flooding of control messages is optimized in order to avoid unnecessary transmissions. For that purpose, each node selects MPRs among its one-hop neighbors. A MPR forwards only the messages from the nodes by which it has been selected as MPR and not the others. The only requirement for the algorithm of choice is that a message relayed by MPRs can reach all the two-hop neighbors of the sender. Figure 3.3 shows an example of OLSR where nodes **A** and **C** are MPRs for node **B**. Notice that nodes **D**, **E**, **F**, **G** and **H** could be selectors for other nodes in the network. A node is informed that it is MPR through "hello" messages from the selector. Also, using hello messages help in the determination whether the link to a neighbor is bidirectional (symmetric) or unidirectional (asymmetric). There are three conditions necessary for a node to relay a message: the message header must indicate that it must be relayed, the message has not already been received by the node, and the node must be MPR of the neighbor having sent the message.
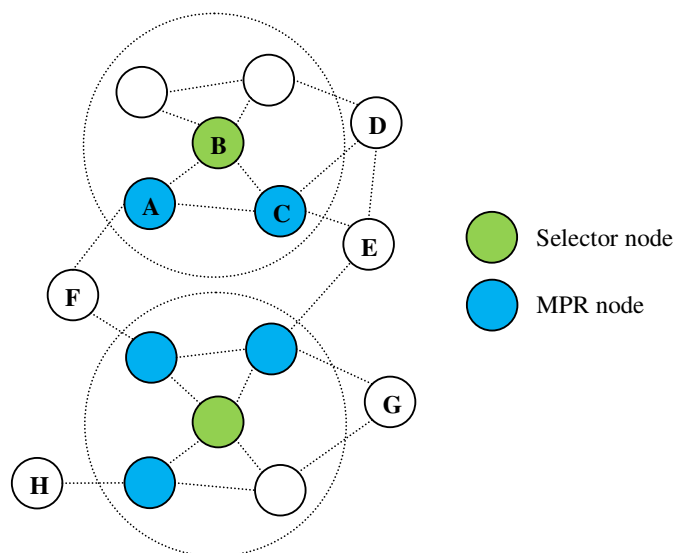
Figure 3.3: Example of OLSR.

All the nodes that are MPR for at least one node periodically broadcast a TC message. A TC message contains the address of the sender and addresses of all the nodes for which it is MPR. By this way all the nodes can make a partial topology graph containing all reachable nodes and the set of links between MPR and their selectors. An algorithm can then calculate the optimum path to any node using that graph. By this way, each node maintains a routing table which allows it to route packets for other destinations in the network. If the graph is changed, the routing table is recalculated to update the route information about each known destination in the network. The main disadvantage of OLSR is the significant control overhead in large networks or in networks with rapidly moving nodes.

3.4 Summary and Conclusions

A choice between proactive and reactive routing protocol has to be made. Proactive approaches have the advantage that routes are immediately available whenever they are requested. However, the main disadvantage of this approach is the addition of significant control overhead in large networks. The benefit of reactive approach is the reduction of the control overhead, particularly in networks with low to moderate traffic loads. However, the primary drawback of reactive approach is the introduction of a high initial latency in packet delivery.

Any of MANET routing protocols can be used in UWB networks. A key aspect to be taken into account is the capability of UWB to provide ranging and positioning information. A routing study performed by UCAN [61] considers positioning information provided by UWB [9]. However, positioning information may not be available at all times. The need to build an initial positioning database at network setup and possible errors and lack of information will eventually cause both ranging and positioning information to be unavailable in some or all terminals. Such terminals should be capable to perform routing as well, even without the advantages offered by positioning information. Another key aspect to be taken into account is the large channel capacity of UWB technology. Therefore, routing overhead can be acceptable to a certain extent in UWB ad hoc networks. However, delay in establishing routes could prevent nodes from utilizing this large capacity.

Such considerations lead us to think of a routing protocol that makes use of the large capacity of UWB technology to enhance routing performance. That is, we should develop routing mechanisms that will reduce time of route establishment even if this will increase routing overhead to a certain extent. Therefore, a study on the modifications and adaptations required to adopt such a protocol in a UWB MANET is needed. In the next Chapter, we define and describe our simulated network scenario and present a performance evaluation of three popular MANET routing protocols in order to specify the basic requirements needed to design a suitable routing protocol for our network scenario.

4 NETWORK SCENARIO AND PERFORMANCE EVALUATION

In this Chapter, we define and describe the simulated network scenario which represents an industrial indoor application that uses UWB technology. A viable industrial indoor application is a production line in a factory. In this application, UWB technology can be applied since it is suitable for indoor applications because of its robust performance in noisy environments. The investigations were accomplished through the simulation software. In these investigations, a performance evaluation of AODV, DSR and OLSR was carried out. A paper was published based on these investigations [6].

4.1 Network Scenario

A production line is a set of sequential operations established in a factory by which materials are put through a refining process to produce an end-product that is suitable for onward consumption; or components are assembled to make a finished article [64]. Our network scenario represents a production line in a factory. The production line consists of two main components: materials boxes moved by a conveyor belt and machines that manipulate the materials. In order to control the production process, it is intended to interconnect the machines with each other through the moving material boxes. Consequently, a multi-hop MANET is formed. The links between nodes are bidirectional and established using UWB technology. In this thesis, line topology is used since it is the common topology used in factories nowadays. Along the production line, material boxes are distributed uniformly. Uniform distribution may not be the most realistic choice but we use it for illustrative purposes in order to establish a rough basic understanding of such network scenario.

As shown in Figure 4.1, the network consists of fixed nodes (machines) and mobile nodes (material boxes) distributed along a linear topology at regular distances, i.e., uniform distribution. Distance between fixed nodes is basically 30m, while distance between mobile nodes is varied from 1 to 30m. The mobile nodes are moving from one side to the other with constant speed of 1m/s. We assume that there are always mobile nodes along the production line. As a mobile node exits the production line from one side, a new mobile node enters the production line from the other side. The network size is varied from 2 to 9 fixed nodes and number of mobile nodes depends on the distance between them.
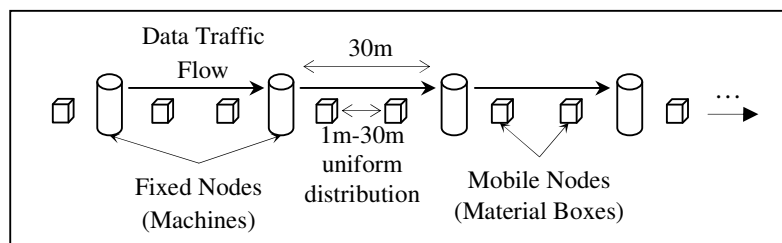

Figure 4.1: Production Line Topology.

Each fixed node sends basically one data packet to the next fixed node (in direction of movement) every 30s using Transmission Control Protocol (TCP) connections. The size of this data packet is 1024 bytes and it contains information (codes numbers) about the mobile

nodes moving between the two fixed nodes. In other words, there is one data traffic flow between each two successive fixed nodes with data rate of 0.27Kb/s that we will call it the basic data rate. Notice that the basic data rate is calculated here at the application level excluding protocol overhead, and excluding retransmitted data packets. This data rate is sufficient to control the manufacture process and it is low enough to be used in 802.15.4a-like networks within a noisy environment.

4.2   Simulation Environment

The well-known network simulator ns-2 [45] has been used in this thesis. Ns-2 is designed for networking research and it covers a very large number of applications, protocols, network types, network elements and traffic models. Ns-2 is an open source software package available for both Windows [38] and Linux [30] platforms. It has many expanding deployments including:

- performance evaluation of existing network protocols,
- evaluation of new network protocols and technologies before real implementation,
- execution of large scale experiments not possible in real experiments.

Ns-2 consists of object oriented modules written in C++ [49] and an interpreter used to execute user's command scripts. The interpreter language is Object Tool Command Language (OTcl) [35]. In other words, there are two class hierarchies: the compiled C++ and the interpreted OTcl. The compiled C++ hierarchy enables the simulation to achieve efficient and fast execution times. This is in particular useful for detailed definition and operation of protocols and network elements. In OTcl script, the user can define the network topology with the specific protocols and applications, and the form of the output that he wishes to obtain from the simulator. The Otcl can make use of the objects compiled in C++ through an OTcl linkage that creates a matching OTcl object for each of the required C++ objects.

Ns-2 is a discrete event simulator in which the timing of events is maintained by a scheduler. An event is an object in the C++ hierarchy with unique ID, a scheduled time and the pointer to an object that handles the event. The scheduler keeps an ordered data structure with the events to be executed and fires them one by one, invoking the handler of the event. We refer the reader to [2], [35] and [46] for full description of this simulator.

The production line scenario was simulated using ns-2 version ns-allinone-2.29.3 running under SUSE Linux 10.1 operating system. Experiment simulation time was 750s including a warming up period of 150s. All packets exchanged during this period were discarded and not included in computations. Thus, the actual simulation time was 600s. To achieve a reasonable confidence interval, each simulation experiment was repeated 50 times and their average was used. Our simulation software is freely available [56]. Also, our institute IKT will be provided with a copy of the simulation software on a Compact Disk (CD).

4.2.1   UWB PHY and MAC Layers

The shadowing model described in section 2.4 was used to reflect UWB pathloss model in the PHY layer. Since our network scenario represents an industrial indoor application, the values of PL_o, β and σ_s are 56.7dB, 2.15 and 6dB respectively according to the final report of UWB

channel model provided by IEEE 802.15.4a [39]. The shadowing model with a joint PHY/MAC architecture for an 802.15.4a-like UWB MANET is implemented in ns-2 [36] and the code version ns-2.29-uwb-0.10.0 was used [63]. This architecture is based on TH-IR-UWB system with three main components: interference mitigation; dynamic channel coding that continuously adapts the transmission bit rate to variable channel conditions and interference; and MAC that resolves contention for the same destination. We refer the reader to [37] for full description of this architecture.

The transmission bit rate is variable (1.8Mb/s – 18Mb/s) since it depends on the channel code being used [37]. The transmission range of nodes is also variable since it depends on channel coding [36]. Moreover, the transmission range of a node is not constant in all directions (not a circle) as discussed in 2.4. In our simulation experiments, the transmission range was found to be in the range from 5m to 15m. Therefore, the average transmission range of UWB nodes was around 10m in our network scenario. Center frequency was 5GHz and bandwidth was 1GHz. The average transmission power was 1μW.

To justify the use of UWB technology in multi-hop MANET, WLAN model operating with IEEE 802.11a standard [59] was also used in the same frequency band, transmission bit rate and shadowing model as in UWB MANET. Notice that we assumed in our network scenario that the maximum distance between machines (fixed nodes) is 30m. At this range, WLAN may offer a direct link between machines. Therefore, we reduced the average transmission power of WLAN nodes in order to obtain similar average transmission range as UWB nodes, i.e., around 10m. By this way, we can investigate the multi-hop effect on WLAN in our network scenario. This may look unfair for the first instant. However, the main source of noise in spread-spectrum systems comes from interference of other nodes. Reducing transmission power will reduce interference power in the network as well. Therefore, signal to interference ratio will stay the same in the network.

4.2.2 Routing Protocols

As clarified in Chapter 3, we considered AODV, DSR and OLSR protocols in our study. The above used version of ns-2 supports AODV and DSR. However, OLSR is not implemented in that version. Therefore, we used the UM-OLSR implementation version 0.8.8 [62].

4.3 Performance Evaluation

In the production line scenario, we compared the performance of AODV and OLSR in our network scenario using UWB and WLAN technologies. Also we compared the performance of AODV, DSR and OLSR in the network scenario using UWB technology. We have used three performance metrics:

- Packet Delivery Ratio (PDR),
- Normalized Throughput (NTh) and
- Routing Overhead Ratio (ROR).

PDR is the ratio between the total received data packets without duplication to the total sent data packets at transport level. NTh is the ratio between the useful received data packets (without duplication and retransmissions) to the total useful data packets that should be

transmitted during the actual simulation time at application level. ROR is the ratio between the cumulative sum of bytes of all routing packets exchanged in the network in order to send data packets to the cumulative sum of bytes of these routing packets and all sent data packets at routing level. PDR and NTh are important metrics for best-effort communications, while ROR metric evaluates routing protocol efficiency.

In addition to the performance metrics, the following ratios (with respect to the total useful data packets that should be transmitted during the actual simulation time at transport level) have been used:

- Received data packets ratio,
- undelivered data packets ratio,
- retransmitted data packets ratio and
- duplicated data packets ratio.

Received data packets ratio indicates the actual amount of useful data packets that are received correctly. Undelivered data packets ratio indicates the rest amount of useful data packets dropped by the sender at the end of simulation because they could not be delivered until that time due to link breaks. Retransmitted data packets ratio indicates the amount of received data packets that are retransmissions of other data packets because some data packets are received but could not be acknowledged in time due to link breaks. Duplicated data packets ratio indicates the amount of received data packets that are repeated copies of other received data packets. These ratios are mainly affected by link breaks in the network and the way by which these link breaks are resolved. Therefore, these ratios can be used in the evaluation of routing protocols efficiency.

For clarity reasons, the simulation results were plotted in smoothed curves using 5-points moving average filtering method implemented in the function *smooth* of MATLAB [34] version 7.4.0.287 (R2007a). For each curve, the 90% confidence intervals [58] including the error introduced by smoothing method were plotted as well. In the following subsections we discuss the simulation results.

4.3.1   Multi-hop Investigation

Here we describe the multi-hop effect on NTh of AODV and OLSR in the production line scenario using UWB and WLAN technologies. To do so, a simple production line with one data traffic flow was used as shown in Figure 4.2. The network consists of two fixed nodes and mobile nodes moving from one side to the other. The mobile nodes are uniformly distributed. The distance between fixed nodes is varied to take the values 10m, 20m and 30m. For each of these values, the distance between mobile nodes is varied from 1m to 30m with 1m step increment. Length of the production line equals to the distance between the two fixed nodes (10m, 20m or 30m) plus 30m before the first fixed node and 30m after the second fixed node. Therefore, number of mobile nodes in the network is variable and it is between 3 and 90 nodes depending on the distance between fixed and mobile nodes. Data traffic consists of only one flow between the two fixed nodes with the basic data rate of 0.27Kb/s. As mentioned before, we adjusted the average transmission power of WLAN nodes in order to obtain similar average transmission range as UWB nodes, i.e., around 10m. The results are shown in Figure 4.3 and Figure 4.4.
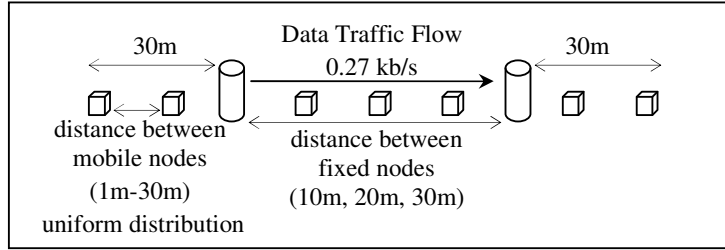
Figure 4.2: Production Line with One Fixed Data Traffic Flow.

Figure 4.3: Multi-hop Effect on NTh of AODV.

When the distance between the two fixed nodes is 10m, the communication between them is done mainly in one hop (direct connection link) since the two fixed nodes are within the coverage area of each other. As shown in Figure 4.3(a), the effect of high density of nodes appears clearly in UWB because the used MAC model is more sensitive to the interference level than MAC model of WLAN (see section 4.2.1). Large distance between mobile nodes means low node density, and thus low interference level. As the distance decreases, the nodes density increases and this leads to higher interference level. This explains why NTh in UWB decreases as the distance between mobile nodes is being decreased, especially when the distance between mobile nodes is smaller than 10m as shown in Figure 4.3(a).

23

When the distance between the two fixed nodes is 20m, they need at least another node between them to establish communications between them because they are outside the coverage area of each other. Therefore, the communication between the two fixed nodes is done mainly in two hops and the multi-hop effect on NTh obviously appears. As shown in Figure 4.3(b), NTh maximum occurs at the transmission range of the nodes, which is found to be around 10m in this experiment. When the distance between mobile nodes is smaller than the transmission range, there are extra nodes than what are needed for multi-hop communications and this leads to higher interference level and control packet overhead. Thus NTh decreases for both UWB and WLAN. As the distance between mobile nodes becomes larger than the transmission range, there are insufficient nodes for multi-hop communications. Accordingly, NTh decreases also in this case for both UWB and WLAN.

When the distance between the two fixed nodes is increased to 30m, the communication between them is done mainly in three hops. Figure 4.3(c) shows clearly that UWB technology achieves a much better NTh than WLAN technology in multi-hop communications with hop count larger than two.

In the previous simulation experiments, one may say that it is not needed to let distance between mobile nodes larger than distance between fixed nodes. That is, when the distance between fixed nodes is 10m, the distance between mobile nodes should be varied from 1m to 10m only. Also, when the distance between fixed nodes is 20m, the distance between mobile nodes should be varied from 1m to 20m only. This is true in case of 10m distance because communications between fixed nodes is done directly between them without the need of any mobile node. However, this is not true in case of 20m distance because the communications between the fixed nodes is done through the mobile nodes between them.

When the distance between mobile nodes is larger than 20m, there will be a period of time in which there is no mobile nodes between the fixed nodes, and hence, no communications between them. However, when a mobile node enters between the two fixed nodes and reaches almost half the way between them (about 10m from each fixed node), a connection between the two fixed nodes is established through the mobile node for a certain time. When the mobile node goes away from the half way, the connection between the fixed nodes will break again. This explains why NTh of UWB does not fall to zero when the distance between mobile nodes is larger than 20m. However, as distance between mobile nodes gets much larger than 20m, the period of time in which there is no connection between the fixed nodes increases, and Thus NTh decreases as shown in Figure 4.3(b).
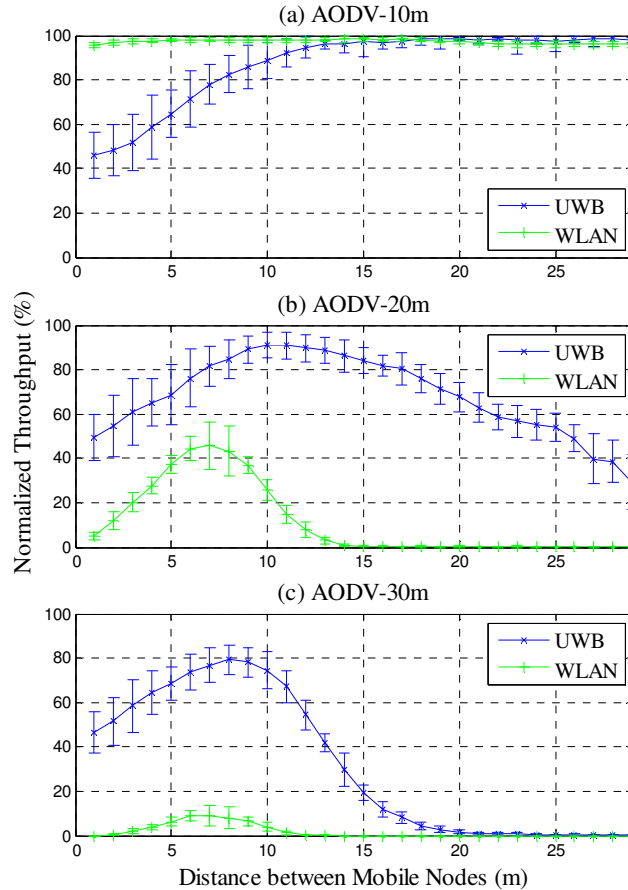
Similar results are obtained when OLSR is used as shown in Figure 4.4. When the distance between the two fixed nodes is 10m, the communication between them is done mainly in one hop. The effect of nodes density appears clearly in UWB especially when the distance between mobile nodes is smaller than 5m as shown in Figure 4.4(a). When the distance between the two fixed nodes is set to 20m and 30m, the effect of multi-hop communications appears clearly as shown in Figure 4.4(b) and Figure 4.4(c). NTh maximum occurs at the transmission range of the nodes, which is found to be around 5m in this experiment. When the distance between mobile nodes gets smaller or larger than the transmission range, NTh decreases for both UWB and WLAN.
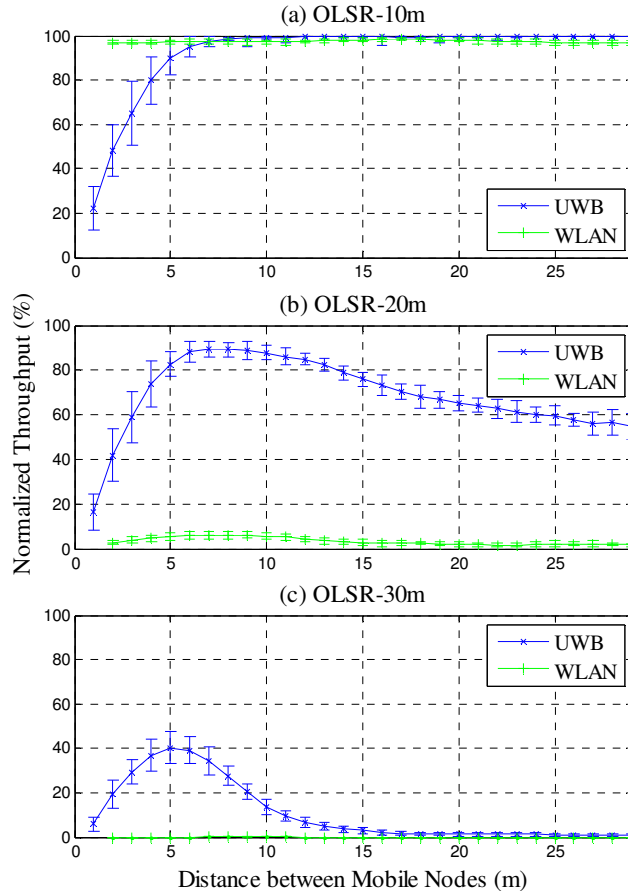
Figure 4.4: Multi-hop Effect on NTh of OLSR.

When comparing Figure 4.3 with Figure 4.4, we see that NTh achieved using AODV is larger than NTh achieved when using OLSR for both UWB WLAN technologies. As mentioned in Chapter 3, AODV is a reactive protocol while OLSR is a proactive protocol. Therefore, OLSR impose much larger routing overhead than AODV. Large routing overhead consumes network capacity, and hence, NTh decreases dramatically. For example, in case of AODV in Figure 4.3(c), maximum NTh is around 80% for UWB and around 10% for WLAN. On the other hand, in case of OLSR in Figure 4.4(c), maximum NTh decreases to about 40% for UWB and almost 1% for WLAN.

Finally, it is obvious from Figure 4.3 and Figure 4.4 that UWB technology achieves a much larger NTh than WLAN technology in multi-hop communications. This justifies the use of UWB technology in our network scenario. The mathematical model for the channel capacity of the production line scenario developed in the next chapter will explain why there is a big difference in NTh between UWB and WLAN technologies.

4.3.2 Data Rate Investigation

The production line with one data traffic flow shown in Figure 4.5 was used to investigate the data rate effect on the performance of AODV, DSR and OLSR based on UWB technology. The network consists of two fixed nodes and mobile nodes moving from one side to the other. The mobile nodes are uniformly distributed. The distance between the two fixed nodes is set

permanently to 30m, while the distance between mobile nodes is varied from 1m to 30m with 1m step increment. Therefore, number of mobile nodes in the network is variable and it is between 3 and 90 nodes depending on the distance between mobile nodes. Length of the production line is 90m. Data rate of the data traffic flow is varied by sending one data packet of size 1024 bytes from one fixed node to the other every 30s (0.27Kb/s), 10s (0.82Kb/s), and 5s (1.64Kb/s). The results are shown in Figure 4.6, Figure 4.7 and Figure 4.8. Furthermore, data packets distribution ratios, with respect to the total useful data packets that should be transmitted, are shown in Figure 4.9, Figure 4.10 and Figure 4.11 in the cases of AODV, DSR and OLSR respectively. These distribution ratios are used to explain some simulation results.
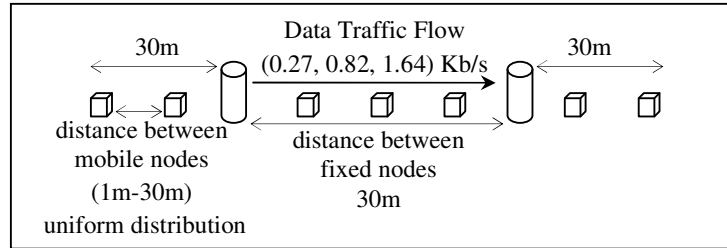
Figure 4.5: Production Line with One Variable Data Traffic Flow.

Let us first discuss the general shape of the curves for PDR, NTh and ROR in Figure 4.6, Figure 4.7 and Figure 4.8. Since the distance between the two fixed nodes is 30m, the communications between them is achieved through multi-hoping. The maximum of PDR and NTH and the minimum of ROR occur when the distance between mobile nodes equals to the transmission range of the nodes because number of mobile nodes used in multi-hopping in this case is optimal. When the distance between mobile nodes becomes smaller than the transmission range, there are extra nodes than what are needed for multi-hop communications and this leads to higher interference level. Therefore, PDR and NTh start to decrease and ROR starts to increase. On the other side, when the distance between mobile nodes becomes larger than the transmission range, there are insufficient nodes for multi-hop communications. In this case also PDR and NTh start to decrease and ROR starts to increase.

Using curves maxima and minima, we can determine the transmission range of the nodes. It is obvious from Figure 4.6, Figure 4.7 and Figure 4.8 that the transmission range of the nodes is not the same for the three routing protocols. It is around 9m for AODV, 11m for DSR and 5m for OLSR. This is because the joint PHY/MAC architecture of UWB that is implemented in ns-2 is based on dynamic channel coding that continuously adapts the transmission bit rate to the variable channel conditions and interference. Transmission bit rate varies from 1.8Mb/s to 18Mb/s depending on the channel code being used [37]. As a result, the transmission range of the nodes is also variable since it depends on the transmission bit rate being used [36]. Each routing protocol has its own effect on channel conditions because of routing overhead introduced to the traffic. Thus, the adopted transmission bit rate will not be the same for all routing protocols, and hence, the transmission range of nodes will not be the same also. For the same routing protocol, curves maxima and minima occur almost at the same points. But, in case of DSR, ROR minima occur at around 17m while PDR and NTh maxima occur around 11m. This is because DSR uses source routing. In source routing, header size of routing control packets depends on path length. Thus, routing control packets have different sizes in DSR. As a result, ROR curves of DSR have not smooth shapes as those of AODV and OLSR. Hence, ROR minima of DSR do not occur accurately as those of AODV and OLSR.

26

Figure 4.6: Data Rate Effect on PDR of Three Routing Protocols.

Figure 4.7: Data Rate Effect on NTh of Three Routing Protocols.
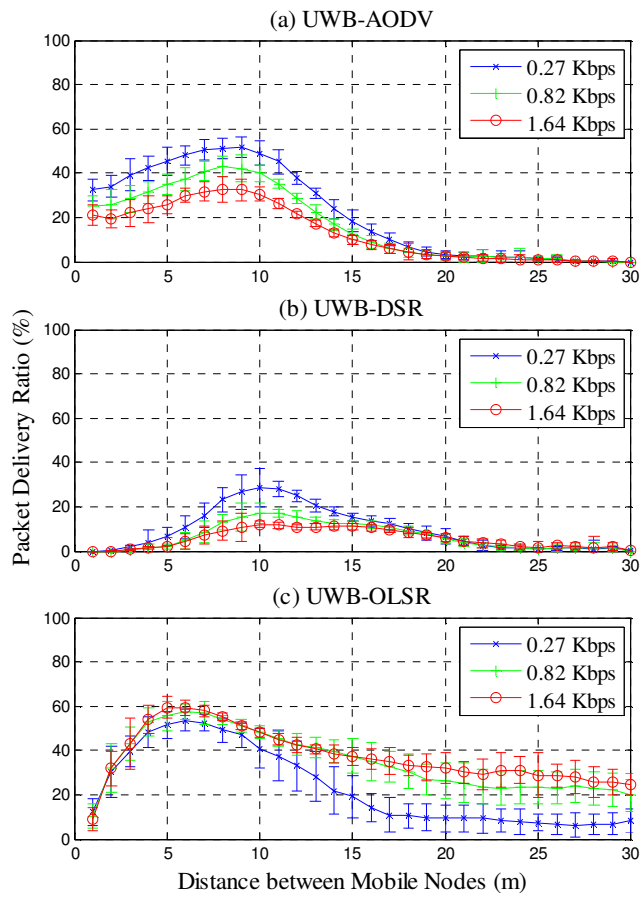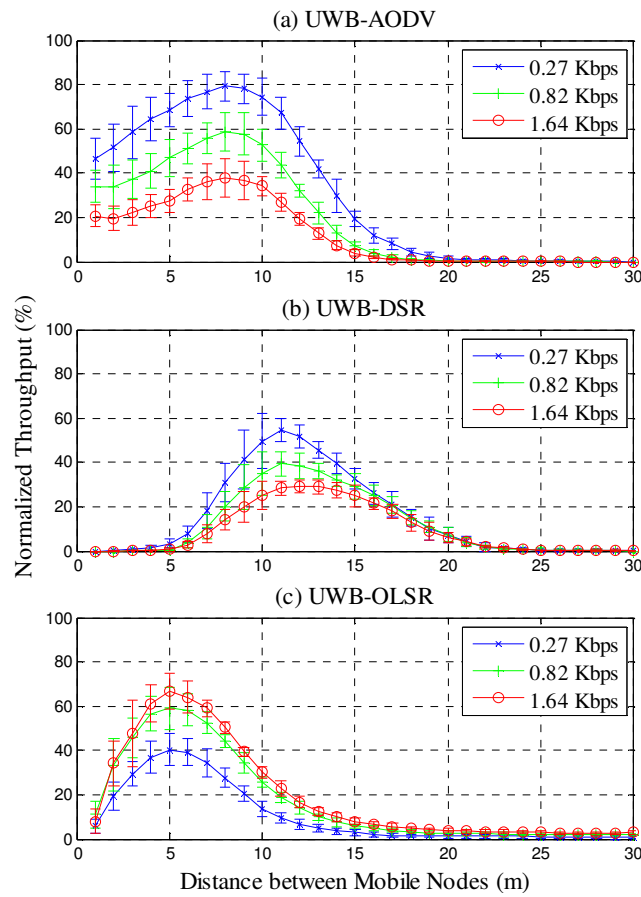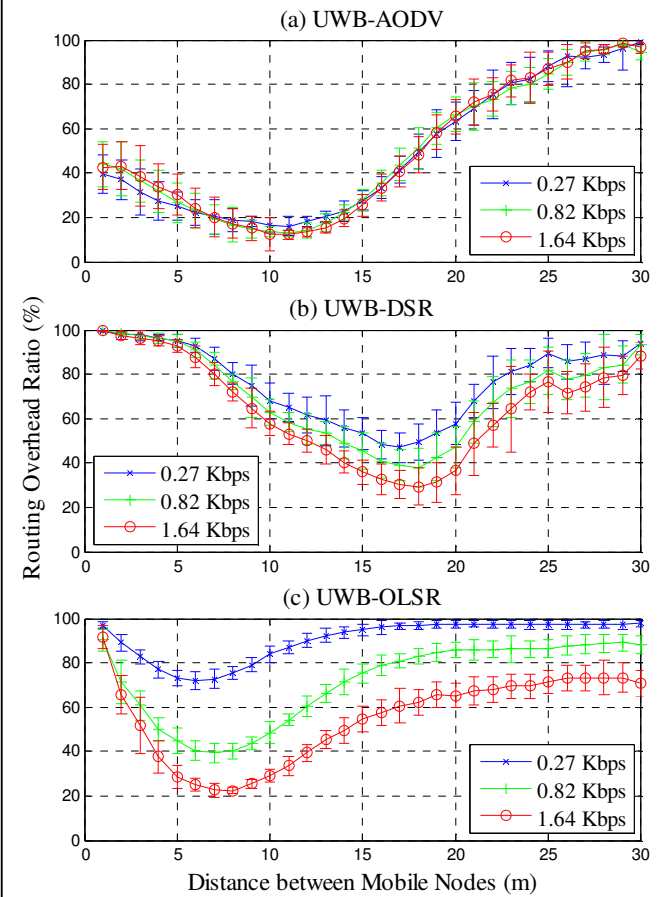
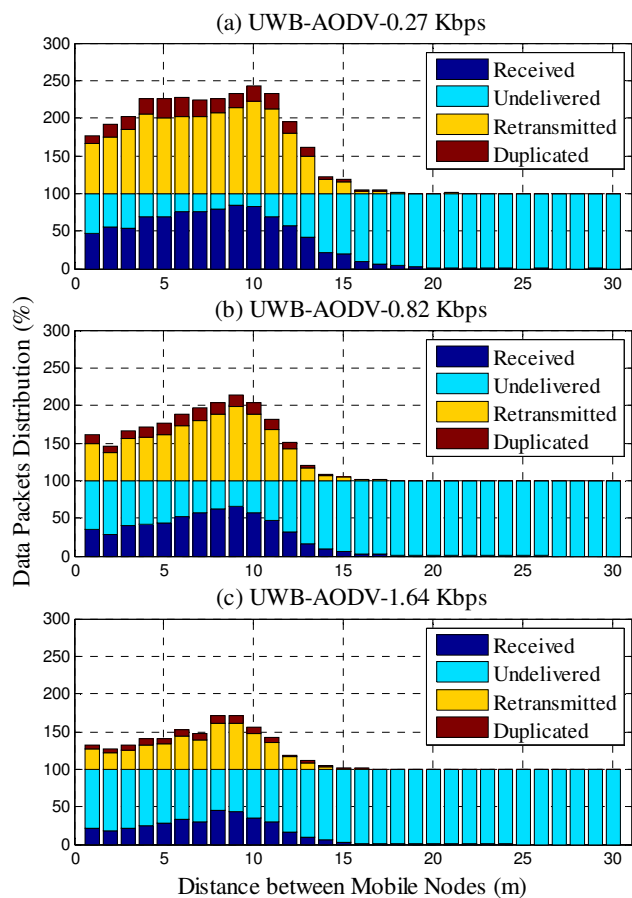Figure 4.8: Data Rate Effect on ROR of Three Routing Protocols.

Figure 4.9: Data Rate Effect on AODV Data Packets Distribution.
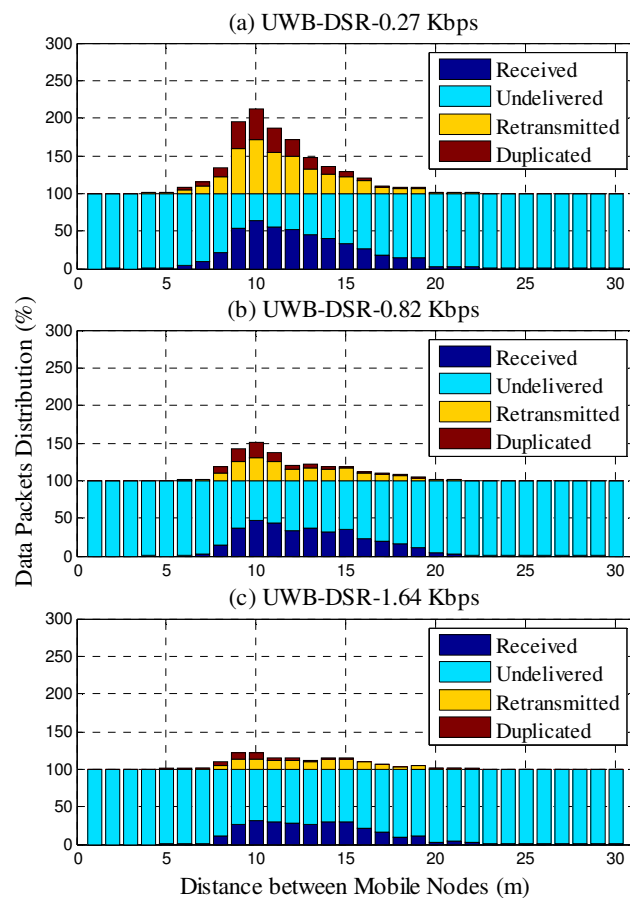

Figure 4.10: Data Rate Effect on DSR Data Packets Distribution.
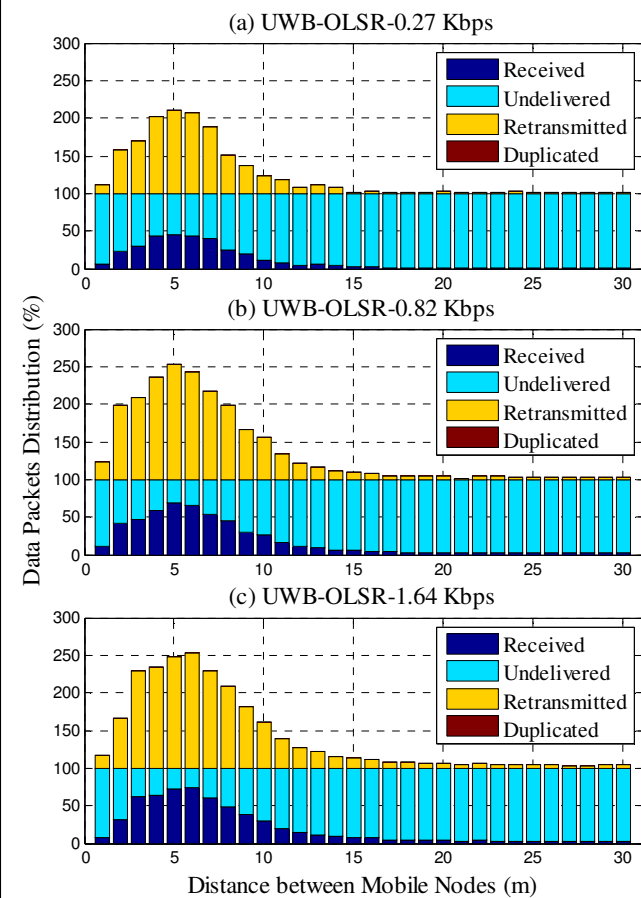

Figure 4.11: Data Rate Effect on OLSR Data Packets Distribution.

Let us now discuss what happens to PDR, NTh and ROR when data rate is increased. Hereafter, we will refer to the region where the distance between mobile nodes is smaller than the transmission range as the region of high node density. Also, we will refer to the region where the distance between mobile nodes is larger than the transmission range as the region of low node density. Unless otherwise stated, we discuss the curves and results around the transmission range region of each routing protocol. Notice that data rate used here is achieved by sending one data packet every 30s (0.27Kb/s), 10s (0.82Kb/s), and 5s (1.64Kb/s). Even for the highest data rate, 5s is relatively long time in which all mobile nodes move 5m along the production line. This means that the route table of the fixed node should be updated each time a packet is sent in case of reactive protocols. With higher data rates, data packets are sent more frequently. In the case of AODV which is a reactive protocol, this will lead to initiate more route discovery and maintenance procedures. As more route procedures become vulnerable to link breaks, more data packets are not delivered since they need to wait until a route is established. Hence, as data rate increases, the ratio of undelivered data packets increases as shown in Figure 4.9. This is reflected in lower PDR as seen in Figure 4.6(a). As a result, NTh in Figure 4.7(a) decreases as data rate increases. The same behavior is noticed in case of DSR for PDR, NTh and data packet distribution as shown in Figure 4.6(b), Figure 4.7(b) and Figure 4.10 respectively.

In contrast, in the case of OLSR, routing tables are always available and they are maintained continuously regardless of data rate since OLSR is a proactive protocol. Hence, data packets are sent immediately and need not to wait until a route is discovered. Consequently, as data rate increases more data packets are delivered (received and retransmitted data packets ratios increase) as shown in Figure 4.11. As a result, as long as network size is unchanged, PDR and NTh increase as data rate increases as shown in Figure 4.6(c) and Figure 4.7(c) respectively.

Notice also that when the distance between mobile nodes is larger than 15m (low node density region), PDR of OLSR in Figure 4.6(c) increases more obviously as data rate increases, e.g., at 25m PDR is around 7% for 0.27Kb/s and it increases to 30% for 1.64kb/s. This behavior is not noticed in PDR of AODV and DSR in Figure 4.6(a) and Figure 4.6(b) because with higher data rate PDR decreases as mentioned before. Also, this behavior is not noticed in NTh of OLSR itself as shown in Figure 4.7(c) because NTh is calculated at application level, while PDR is calculated at transport level. Therefore, the behavior of PDR should not be the same as NTh. This explains why as data rate increases, the increase in NTh is not obvious as that of PDR when the distance between mobile nodes is larger than 15m.

By comparing ROR of the three routing protocols shown in Figure 4.8, it is found that AODV has the lowest ROR, particularly for low data rate. But AODV tends to use route discovery and maintenance procedures frequently. Therefore, as the amount of data packets increases in the network, more routing packets are generated as well, and thus the ratio between routing packets and data packets represented by ROR is not affected by the increase of data rate and it remains almost at the same level in the case of AODV as shown in Figure 4.8(a). On the other hand, DSR and OLSR have different behaviors. DSR does not tend to use frequent routing procedures since it stores multi-routes in its route cache for the same destination. Therefore, an increase in data packets will not result in a same relative increase ratio in routing packets. Therefore, as data rate increases, ROR of DSR decreases as shown in Figure 4.8(b). In the case of OLSR, the routing tables are built proactively. For the same number of nodes (network size does not change as data rate increases), the same routing tables are built

independently from the data rate even if there is no data packet to send. This explains why ROR of OLSR decrease as data rate increases as shown in Figure 4.8(c).

AODV outperforms DSR in this scenario. This is because DSR has no mechanism to delete out-of-date routes from its route cache. Also, DSR uses source routing and this increase the size of control packets. As a result, a very low delivery ratio of data packets (received ratio) is noticed in Figure 4.10. Thus, DSR has much lower PDR and much higher ROR, which leads to lower NTh as shown in Figure 4.6, Figure 4.8 and Figure 4.7 respectively. Also in this scenario, AODV outperforms OLSR in the case of low data rate. As data rate increases (while keeping network size unchanged), OLSR begins to outperform AODV in terms of PDR and NTh as shown in Figure 4.6 and Figure 4.7 since it is a proactive protocol. Moreover, at high data rates, ROR of OLSR is expected to be lower than that of AODV as Figure 4.8 shows.

A final observation on the general shape of the curves for PDR, NTh and ROR in Figure 4.6, Figure 4.7 and Figure 4.8 is that as data rate increases, the increase (or decrease) ranges of PDR, NTh and ROR are not the same for the same routing protocol. For example, in case of AODV in Figure 4.6(a), Figure 4.7(a) and Figure 4.8(a) at 8m, as data rate increases from 0.27kb/s to 1.64kb/s, PDR decreases from about 55% to 35% (decrease range is 20%), NTh decreases from about 80% to 40% (decrease range is 40%) and ROR stay almost unchanged (decrease range is almost 0). The reason for these different ranges for the same routing protocol is that each parameter is calculated at different level. PDR is calculated at transport level, NTh is calculated at application level and ROR is calculated at routing level.

Let us now focus on data packets distribution ratios shown in Figure 4.9, Figure 4.10 and Figure 4.11 in cases of AODV, DSR and OLSR respectively. These ratios are calculated at transport level. Received ratio indicates the actual amount of useful data packets that are received correctly. Undelivered ratio indicates the rest amount of useful data packets dropped by the sender at the end of simulation because they could not be delivered until that time due to link breaks or congestion. As shown in the three figures, the summation of received and undelivered ratios equals to 100%. This is expected because if the sender is given enough time, it will send all data packets since TCP guarantees packet delivering. Retransmitted ratio indicates the amount of received data packets that are retransmissions of other unacknowledged received data packets due to link breaks. Retransmissions cannot be avoided in ad hoc networks since link break is a common feature of it. Duplicated ratio indicates the amount of received data packets that are repeated copies of other received data packets. Duplications occur when the same packet is sent unexpectedly using different paths.

Another observation noticed is the large amount of data retransmissions in case of the three protocols, and the small amount of data duplication in case of AODV and DSR as shown in Figure 4.9, Figure 4.10 and Figure 4.11. This is due to the frequent link breaks occurring in the network. Notice that data retransmissions increases when the received data increases. In case of AODV and DSR, data retransmissions are more obvious at low data rates because as data rate increases, the amount of received data packets decreases. In case of OLSR, data retransmissions are more obvious at high data rates because as data rate increases, the amount of received data packets increases.

One more remarkable observation is that there is no data duplication in the case of OLSR as shown in Figure 4.11. This is because routing mechanisms in OLSR are more controllable

since packets are not flooded by any node (as in AODV and DSR), but only by MPR nodes. Thus, OLSR has more reliable route paths. As a result, OLSR is protected against data duplication by limiting number of forwarding nodes and centralizing some routing tasks.

Finally, the extra retransmissions and duplications are considered as an additional useless overhead that consumes network capacity. For example, in Figure 4.9(a) at distance 10m between mobile nodes, almost 80% of useful data packets are received. However, in addition to these useful data packets, there are about 140% of data packets (summation of retransmitted and duplicated ratios) are received as retransmissions and duplications of other data packets. These extra retransmissions and duplications along with routing overhead of the routing protocol contribute in consuming network capacity and resources. Therefore, reducing data packets retransmissions and duplications should be taken into account when designing a routing protocol.

4.3.3 Scalability Investigation

Here we describe the scalability of AODV and OLSR in the production line scenario using UWB technology. Production lines with one, three and eight data traffic flows were used. Figure 4.12 shows production lines with one and three data traffic flows. Number of fixed machines equals to the number of flows plus one. That is, the network consists of 2, 4 and 9 fixed nodes when there are one, three and eight data traffic flows respectively. The distance between fixed nodes is always 30m. There are also mobile nodes moving from one side to the other and they are uniformly distributed. The distance between mobile nodes is varied from 1m to 30m with 1m step increment. Number of mobile nodes is variable and it depends on the distance between mobile nodes and the length of the production line. Length of the production line equals to 30m multiplied by number of flows plus 30m before the first fixed machine and 30m after the last fixed machine. Therefore, number of mobile nodes is between 3 and 300. Data traffic consists of only one flow between each two successive fixed nodes with the basic data rate of 0.27Kb/s. The results are shown in Figure 4.13 and Figure 4.14. In addition, data packets distribution ratios, with respect to the total useful data packets that should be transmitted, are shown in Figure 4.15 and Figure 4.16 in the cases of AODV and OLSR respectively. These distribution ratios are used to explain some simulation results.
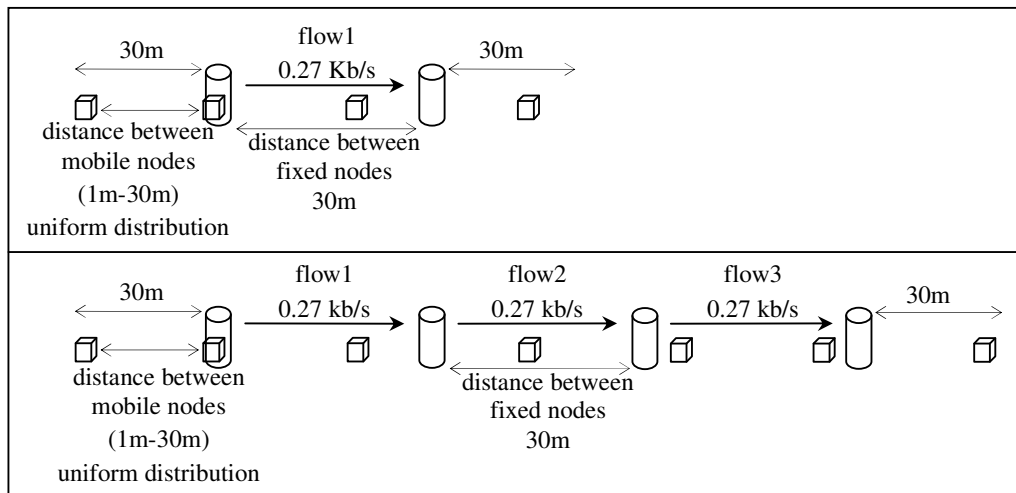

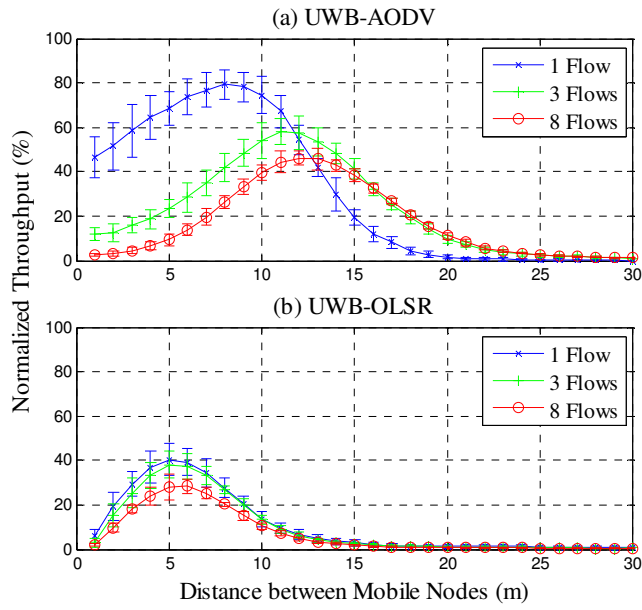Figure 4.12: Production Lines with One and Three Data Traffic Flows.

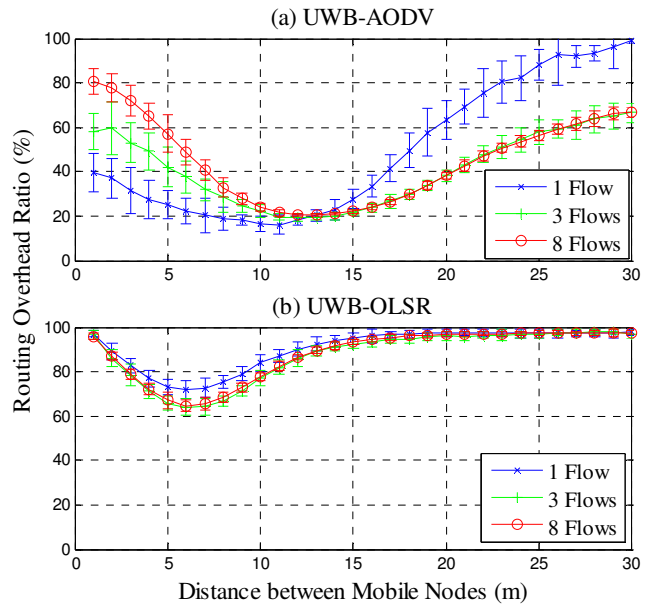Figure 4.13: Scalability Effect on NTh of AODV and OLSR.

Figure 4.14: Scalability Effect on ROR of AODV and OLSR.
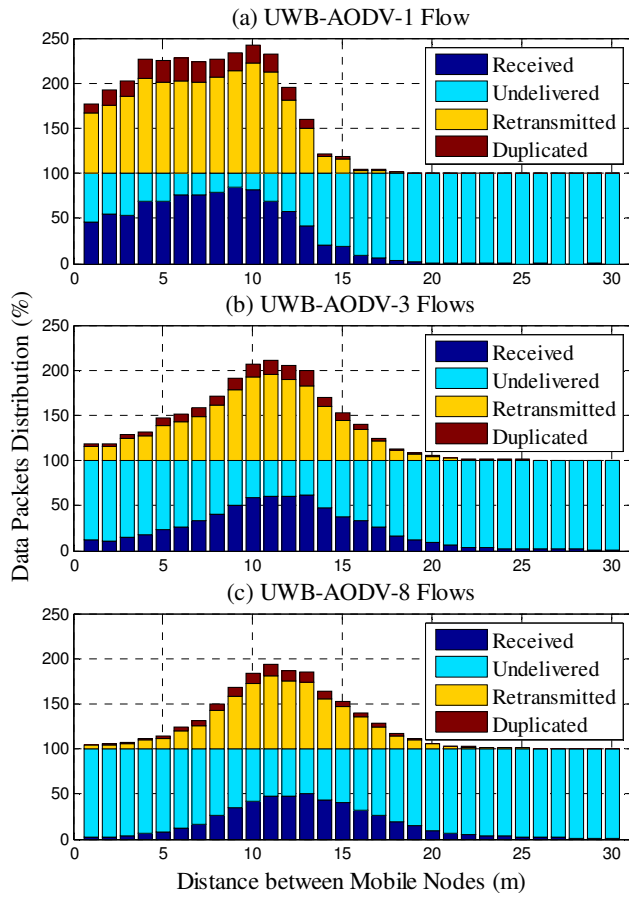
Figure 4.15: Scalability Effect on AODV Data Packet Distribution.
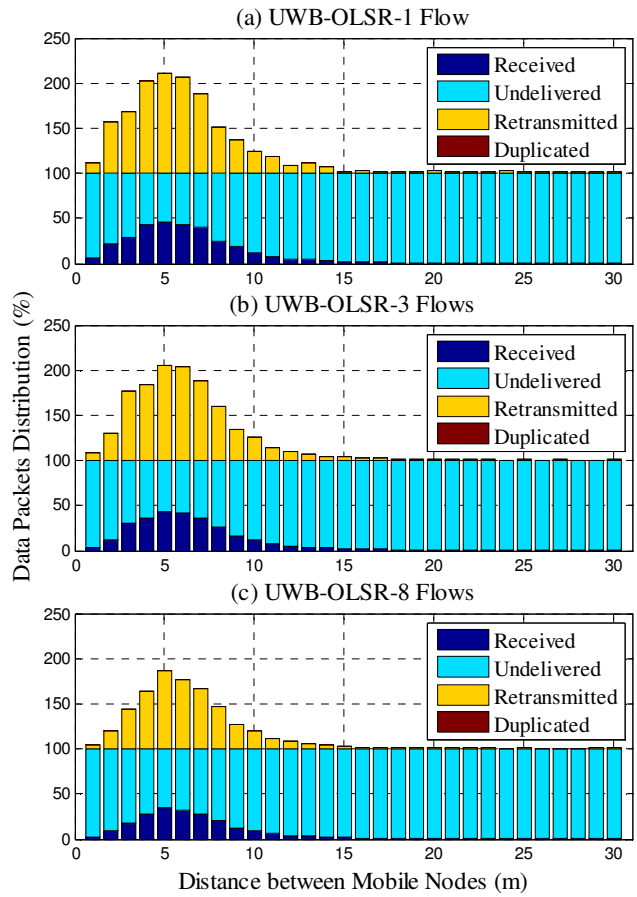
Figure 4.16: Scalability Effect on OLSR Data Packet Distribution.

Again, we would like to remind the reader that in our discussion, we refer to the region where the distance between mobile nodes is smaller than the transmission range as the region of high node density. Also, we refer to the region where the distance between mobile nodes is larger than the transmission range as the region of low node density. Unless otherwise stated, we discuss the curves and results around the transmission range region of each routing protocol.

In this scenario, as flow number increases, number of nodes in the network increases as well. Larger number of nodes leads to higher interference level and thus more frequent link breaks occur. In the case of AODV, as flow number increases, more route procedures are exposed to the link breaks. Hence, as flow number increases, the ratio of undelivered data packets increases as shown in Figure 4.15, and hence NTh decreases at high node density and around the transmission range regions as shown in Figure 4.13(a). However, at low node density and specifically when distance between mobile nodes is larger than 12m, the situation is the opposite, i.e., as flows number increases, NTh increases but it is still lower than the maximum at transmission range distance. This looks abnormal for the first moment. However, this can be simply justified in the following paragraph.

Figure 4.17 depicts our network scenario at a certain time. Assume that the distance between mobile nodes is 22m (distance between fixed nodes is 30m). In the case of one data traffic flow, there is no link between the two fixed machines since the distance between the source node and the mobile node is 22m and NTh is almost zero above 20m, see Figure 4.13(a). This is true also for flow1 in the case of three data traffic flows assuming the same environment conditions. However, for flow2, the mobile node is 14m apart from the source node and 16m away from the destination node. At these distances multi-hop links may exist between the source and destination nodes. Obviously flow3 is impaired since the distance between the mobile nodes is 22m. Therefore, in this example of Figure 4.17, there is no traffic in the case of one data traffic flow, while in the case of three data traffic flows there is traffic due to flow2. This explains why NTh of AODV in the case of one data traffic flow is almost zero at 22m while it is greater than zero in the cases of three and eight data traffic flows as shown in Figure 4.13(a).
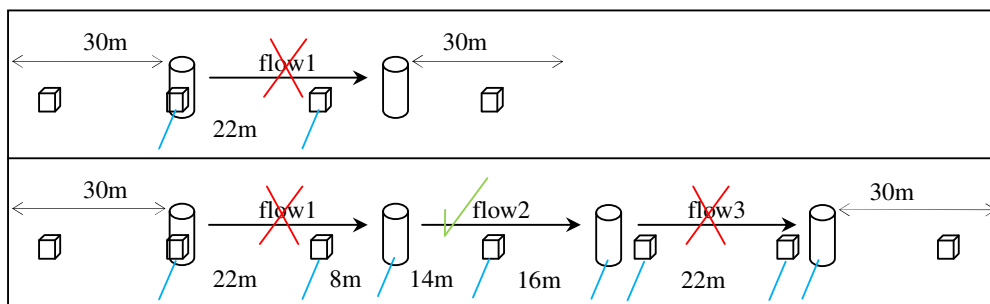
Figure 4.17: Production Lines with One and Three Data Traffic Flows at a certain time.

Let us discuss ROR curve behavior of AODV shown in Figure 4.14(a). As flow number increases since both data traffic and number of nodes increase. As number of nodes increases, routing overhead increases as well. Therefore, as flow number increases, ROR increases at high node density and around the transmission range regions. However, at low node density the opposite is observed. In low node density region, data traffic flows are impaired. As discussed in the example shown in Figure 4.17 where the distance between mobile nodes is

22m, there is no traffic in the case of one data traffic flow, while in the case of three data traffic flows there is traffic due to flow2. This explains why ROR of AODV in the case of one data traffic flow is higher than that in the case of three and eight data traffic flows at low node density.

In the case of OLSR, the variations in NTh and ROR are very small as flows number is increased as shown in Figure 4.13(b) and Figure 4.14(b). Therefore, the conversion in the behaviors of NTh and ROR between low and high node density are not noticeable. Furthermore, as we said before, when flows number increases not only data traffic increases but also number of nodes. As number of nodes increases in the network, each node needs more time to create longer routing tables due to the proactive nature of OLSR. Therefore, routing overhead grows as flows number increases. As a result, ROR of OLSR does not decrease and stays at high levels as shown in Figure 4.14(b). With high ROR, routing control packets consume the network capacity. Hence, as shown in Figure 4.16, the ratio of received data packets decreases as flow number increases. Consequently, as shown in Figure 4.13(b), NTh of OLSR decreases as flow number increases.

Finally, notice the large amount of data retransmissions in case of AODV and OLSR, and the small amount of data duplication in case of AODV as shown in Figure 4.15 and Figure 4.16. This is due to the frequent link breaks occurring in the network. Notice also that data retransmissions increases when the received data increases. In case of AODV, data duplications and retransmissions are more obvious at low flow number because as flow number increases, the amount of received data packets decreases. In case of OLSR also, data retransmissions are more obvious at low flow number. However, there is no data duplication in the case of OLSR as shown in Figure 4.16. This is because OLSR limits number of forwarding nodes and centralizes some routing tasks as discussed before.

4.4 Proposed Approaches for Efficient Routing Protocols

Based on the results discussed in the last section, we propose two approaches to design efficient routing protocols for our network scenario:

- Enhanced (or modified) protocol based on a reactive routing mechanism: routing protocols considered in this study have some routing mechanisms that will lead to better routing performance if they are combined in one routing protocol. In our scenario, the communications between fixed nodes is done mainly in 3 hops. Therefore, by combining source routing with multiple routes per destination (DSR mechanisms) with a time threshold to delete old routes (AODV mechanism), the problem of stale routes (drawback of DSR) will be solved and the need to use frequent route discovery process (drawback of AODV) will be reduced. Also, by controlling some routing tasks such as message flooding (OLSR mechanism), data packet duplication (AODV and DSR drawback) will be eliminated.
- New protocol based on a proactive routing mechanism: This approach needs that the routing protocol will have two phases: transient phase and steady-state phase. In the transient phase, OLSR is used at the start up of the network to build initial routing tables since it is a proactive protocol. Then in the steady-state phase a new protocol that reduces routing overhead should be used. In our scenario, every fixed node is sending information about the moving nodes to the next fixed node regularly.

Therefore, in the steady-state phase, nodes can exploit this information to maintain and update routing tables automatically without the use of extra routing control packets, since the speed and location of mobile nodes can be easily determined in this scenario. As a result, routing overhead for large network size will be decreased (OLSR drawback).

4.5 Summary and Conclusions

Although AODV and DSR are both on-demand ad hoc routing protocols, they differ in their routing mechanisms. AODV uses routing tables, one route per destination, time threshold to delete inactive routes, and destination sequence number to prevent loops and to determine the freshness of a route. On the other hand, DSR uses source routing and cache routes that maintain multiple routes per destination. DSR does not have lifetimes for route cache entries. Once a route is placed in the route cache, it can remain there until it breaks. On the other hand, OLSR is a proactive routing protocol that is optimized by limiting the number of forwarding nodes and centralizing some routing tasks in the network. This is done for two reasons: to reduce routing overhead using MPR node concept by which the information about the 2-hops neighborhood is flooded only; and to increase reactivity to topological changes.

The differences in routing mechanism of AODV, DSR, and OLSR lead to different performance results. After justifying the use of UWB technology instead of WLAN technology in a multi-hop ad hoc network scenario that represents a production line in a factory, a performance comparison of AODV, DSR, and OLSR was carried out. We found that AODV outperforms DSR in our network scenario. In addition, AODV outperforms OLSR in small networks with low data rates (less than almost 1Kb/s). When data rate increases (greater than 1Kb/s) without increasing the network size, OLSR outperforms AODV. However, the performance of OLSR degrades as network size increases and AODV again outperforms it.

Regardless the used routing protocol, the maximum values of PDR and NTh or the minimum value of ROR are achieved when the distance between mobile nodes equals to the transmission range of the nodes. This is because at this distance, number of mobile nodes in the network is optimal for multi-hop communications. If the distance between mobile nodes is smaller than the transmission range, there will be extra nodes than what are needed for multi-hop communications and this leads to higher interference level and control packet overhead. On the other hand, if the distance between mobile nodes is larger than the transmission range, there will be insufficient nodes for multi-hop communications. Therefore, to get a full utilization of the production line network, the distance between materials boxes (mobile nodes) should be adjusted to the transmission range of the nodes.

Two approaches are proposed to design efficient routing protocols for our network scenario. The first approach is based on an enhanced (or modified) protocol with a reactive routing mechanism. This approach is adopted since routing protocols considered in this study have some routing mechanisms that will lead to better routing performance if they are combined in one routing protocol. The second approach is based on a new protocol with a proactive routing mechanism. Using this protocol in our scenario, nodes can exploit the information sent between fixed nodes to maintain and update routing tables automatically without the use of extra routing control packets.

Since our investigations were based on simulation results only, we developed a mathematical model for the channel capacity of the production line scenario as a tool for benchmarking and validation. Also, the big difference in the achieved NTh between UWB and WLAN gave us another reason to develop such a model in order to justify this result. This model is presented in the next chapter.

5 CAPACITY OF AD HOC NETWORKS WITH LINE TOPOLOGY

In this thesis, we focused on channel capacity computation of ad hoc networks with line topology because it is the topology used in our network scenario described in Chapter 4, i.e., a production line in a factory. UWB is a new transmission technique that is supposed to replace WLAN transmission techniques in multi-hop ad hoc networks in short range scenarios. Hence, a systematic model was used to find closed-form formulas for the channel capacity of ad hoc networks with line topology based on UWB and WLAN technologies. These formulas can be used as a tool for benchmarking and validation of our simulation results obtained in Chapter 4. A paper was published based on results presented in this Chapter [5].

In ad hoc networks, communication between nodes is established via wireless links. Nodes can use this link according to a certain medium access scheme. All nodes of ad hoc networks operate as routers to forward packets for other nodes. Thus a multi-hop communications network is formed. In addition, as nodes can move freely, topological changes are very often. Channel capacity is an important parameter in the evaluation and design of ad hoc networks. Analytical computation of channel capacity of ad hoc networks is a very difficult task since it depends on many factors such as channel model, network topology, medium access, routing mechanism and traffic pattern. Thus, some assumptions should be made to simplify mathematical derivation. Good assumptions may lead to results that can be generalized.

In this Chapter, closed-form formulas of the channel capacity are found using a similar procedure like that used in [25]. However, our work here differs mainly in two things. Firstly, we consider a different topology, i.e., the line topology. Secondly, besides considering WLAN technology, we consider also UWB technology. Therefore, our work in this Chapter presents a new contribution in finding a closed-form formula for the channel capacity of UWB MANET with line topology.

5.1 Model Description

5.1.1 Radio Propagation Assumptions

For simplicity of mathematical derivations, we will use the pathloss power law model for radio propagation [50]. In this model, the average power in Watts of a signal at a certain distance d from the transmitter is given by:

$$P(d) = c(d)^{-\beta} \tag{5.1}$$

where β is the pathloss exponent and c is a constant that determines the average power level of transmission. The transmission range of a node denoted by R determines the coverage area of that node. With the power law model, the coverage area of a node is limited by a circle with radius R. A node has a direct link with all other nodes that are positioned within its coverage area.

5.1.2 Topology Assumptions

We will assume that nodes are uniformly distributed along a line topology. Uniform distribution may not be the most realistic choice but we use it for illustrative purposes and to simplify mathematical computations. Figure 5.1 shows our line topology in which each node has 2 adjacent nodes at the same distance Δ with opposite directions. From the view point of node n_0 in the center of line topology, other nodes are placed on the diameter endpoints of co-centered rings, represented by dotted circles, along the same line. The jth ring has a radius of $j \cdot \Delta$ and contains 2 nodes. The size of the network can be expressed in terms of the total number of nodes N, or by K rings around node n_0. N and K are related to each other by:

$$N = 1 + 2K \tag{5.2}$$

$$K = \frac{N-1}{2}; \qquad N \text{ is odd} \tag{5.3}$$
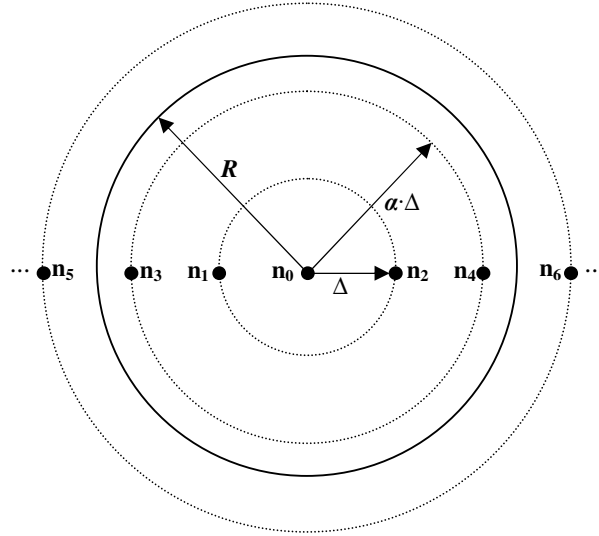
Figure 5.1: Line Topology Configuration.

For example, N is 7 and K is 3 in Figure 5.1. The coverage area of node n_0 is represented by a solid circle of radius R and includes 2 rings as shown in Figure 5.1. The coverage area could be larger and includes more rings. However, the radius R cannot be less than Δ, otherwise, the network would not be connected. We will assume that all other nodes have the same coverage area radius as node n_0. Let α be the number of rings included in the coverage area of a node. For example, α is 2 in Figure 5.1. For fixed R, the density of nodes in the network can be increased by increasing the value of α.

5.1.3 Medium Access Assumptions

On the data link layer, we will assume that the network uses a Medium Access Control (MAC) with Time-Hopping (TH) such as TH-IR-UWB [65]. In this multiple access scheme, all nodes are allowed to transmit simultaneously since a unique TH code is assigned to each node. Even in the lack of synchronization between nodes, collisions are unlikely to occur

since the duty cycle of UWB signal is very small. Hence, all nodes in the network can transmit simultaneously with very low interference level.

For comparison, we will consider also the basic form of the Carrier Sense Multiple Access with Collision Avoidance (CSMA/CA) used in WLAN. According to this multiple access scheme, if a node is transmitting, all other nodes inside the coverage area should not transmit simultaneously [59], i.e., a certain distance (or hop count) between simultaneous transmitting nodes should exist. Thus, the interference level from other nodes will be reduced. However, since only one node can access the channel within a certain coverage area, an additional restriction on channel capacity will be imposed by this MAC protocol [25]. This is mainly related to channel utilization as we will see in section 5.2.

5.1.4 Routing Assumptions

Each node can communicate directly with all nodes inside its coverage area. To communicate with other destinations, multi-hopping must be used. In multi-hop communications there are basically two ways to reach destinations. For example, in Figure 5.1, if node n_0 wishes to communicate with node n_6 on the third ring seen from the center node n_0, it either can hop through node n_2 on the first ring and then node n_4 on the second ring; or it can skip the first ring and hop directly to node n_4 on the second ring before reaching the destination node n_6. The first method conserves energy while the second method keeps the hop-count to a minimum. Our model will consider both methods by controlling the value of α. The energy conservation method is considered if α is 1. Otherwise, the minimum hop-count method is considered.

All rings that can be used for multi-hop routing will be called relay rings and nodes on them will be called relay nodes. Generally, if there are α rings inside the coverage area of node n_0 in Figure 5.1, the number of relay nodes including the source node n_0 is then:

$$N_r = 1 + 2\left\lfloor \frac{K}{\alpha} \right\rfloor \qquad (5.4)$$

where $\left\lfloor \dfrac{K}{\alpha} \right\rfloor$ is the number of co-centered relay rings seen from node n_0 and $\lfloor X \rfloor$ denotes the integer part of X.

5.1.5 Traffic Assumptions

The output traffic per node consists of new traffic that the node generates and relay traffic that the node relays for other nodes. New traffic generated per node will be called the basic throughput per node denoted by r_b. Also, the output traffic per node will be called the output throughput per node denoted by r_o. We will assume that the new traffic is generated by all nodes independently and according to Poisson distribution. It is known that traffic in data packet networks is best represented by heavy-tailed distributions. However, these distributions have complex closed-form formulas. Therefore, Poisson distribution is used for illustrative purposes in order to simplify mathematical calculations. Let λ be the average value of new traffic measured in packet per time-slot t_s per node. t_s is actually the time duration of

one packet and it is determined by the transmission bit rate r (in bits/s) and the packet size P_s at PHY layer (in bits) as following:

$$t_s = \frac{P_s}{r} \tag{5.5}$$

Hence, λ/t_s is the average number of packet transmissions per second. The probability of k packet transmissions during t time interval is then:

$$Pr_k(t, \lambda) = \frac{(t \cdot \lambda / t_s)^k}{k!} exp(-t \cdot \lambda / t_s) \tag{5.6}$$

Let $E[h]$ be the expected hop-count of the network, i.e., it is the average hop-count of all source-destination pairs in the network. A closed-form formula of $E[h]$ will be derived in subsection 5.1.6. For a source-destination pair with $E[h]$ hops between them, there will be an average of $E[h]$-1 relay nodes between them. Therefore, if we assume that there is only one traffic flow between this source-destination pair, the expected amount of relay traffic will be $\lambda(E[h]-1)$. As a result, the average value of the output traffic per node λ_{tot} is:

$$\lambda_{tot} = \lambda + \lambda(E[h]-1) \\ = \lambda \cdot E[h] \tag{5.7}$$

Hence, the probability of packet transmission per node denoted by p_{tr} can be calculated using equation (5.6) as following:

$$p_{tr} = 1 - Pr_0(t_s, \lambda_{tot}) \\ = 1 - exp(-\lambda \cdot E[h]) \tag{5.8}$$

where Pr_0 is the probability of 0 packet transmission (no transmission) during t_s time interval. Finally, r_b and r_o can be related to each other as following:

$$r_b = P_s \cdot \lambda / t_s \\ = \lambda \cdot r \tag{5.9}$$

$$r_o = P_s \cdot \lambda_{tot} / t_s \\ = \lambda \cdot E[h] \cdot r \\ = E[h] \cdot r_b \tag{5.10}$$

From equation (5.10), we can find the maximum allowed basic throughput per node $r_{b,max}$ as following:

$$r_{b,max} = \frac{r_{o,max}}{E[h]} \qquad (5.11)$$

where $r_{o,max}$ is the maximum output throughput per node and it is determined by the channel capacity.

5.1.6   Expected Hop-Count

To find $E[h]$ as a function of number of nodes, the exact hop-count distribution h of the line topology configuration should be found for several network sizes. This is achieved by the procedure listed in Table 5.1 assuming that α=1.

Table 5.1: Calculation of Exact Hop-Count Distribution.

```
1) Begin
2)    input number of rings K
3)    h(1) = 4*K
4)    for i = 2 to 2*K
5)       h(i) = h(i-1) – 2
6)    end
7) End
```

The procedure in Table 5.1 works as following. For a line topology with K rings around the center node and α=1, there will 4K source-destination pairs with hop-count 1 (step 3). The factor of 4 comes from the fact that each ring contains 2 nodes, and each node pair forms 2 source-destination pairs. When hop-count is increased by one (step 4), number of source-destination pairs will be reduced by 2 pairs (step 5). Maximum number of hop-count is 2K (step 4). At the end of this procedure, array h contains the exact number of source-destination pairs that are 1, 2, …, 2K hops apart. For example, when K=2 then $h=\begin{bmatrix} 8 & 6 & 4 & 2 \end{bmatrix}$. This means that there are 8 source-destination pairs with hop-count 1, 6 pairs with hop-count 2, 4 pairs with hop-count 3, and 2 pairs with hop-count 4, as shown in Figure 5.2.
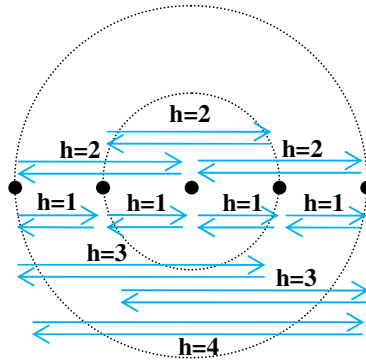
Figure 5.2: Source-Destination pairs in Line Topology with K=2 and α=1.

When h is found, then $E[h]$ can be easily determined. The above procedure is repeated for K=1 ring to K=25 rings, i.e., N=3 nodes to N=51 nodes. For each value of N, $E[h]$ is calculated and it is found to be a linear function of the node number N as described in the following equation:

$$E[h]_{\alpha=1} = \frac{N+1}{3} \qquad (5.12)$$

When $\alpha \neq 1$, equation (5.12) computes the expected hop-count over relay nodes only. When a node that is not on a relay ring needs to transmit, it should first relay its traffic to a node on a relay ring. Therefore, if both source and destination are not on relay rings, $E[h]$ is 2 hops more than the expected hop-count over relay nodes. $E[h]$ is then:

$$E[h] = \frac{N_r+1}{3} + 2\left(1 - \frac{N_r}{N}\right) \qquad (5.13)$$

where N_r is number of relay nodes given in equation (5.4) and ($1-N_r/N$) is the probability that either the source or the destination node is not on a relay ring. Equation (5.13) is valid also when $\alpha=1$ since $N=N_r$ in this case.

5.2   Capacity Calculations

In general, the channel capacity C (in bits/s) between any two nodes in a network is governed by Shannon channel capacity formula [55] that can be expressed in the form:

$$C = W \cdot log_2\left(1 + E[S/I]\right) \qquad (5.14)$$

where W is the channel bandwidth and $E[S/I]$ is the expected value of signal to interference ratio in the channel. However, the used transmission technique and medium access scheme impose some modifications to equation (5.14). A spread-spectrum system needs at least a bandwidth of W determined by the transmission bit rate r, but actually it uses a much larger bandwidth. Using much larger bandwidth will help in reducing the interference power by the processing gain factor g given in equation (2.9).

Medium access scheme will affect the channel capacity in two ways. Firstly, it will restrict the channel capacity by a *channel utilization factor* [25] denoted by u. Secondly, it will affect the calculations of interference in the network. In the following subsections we will find a closed-form formula for the channel capacity using equation (5.14) based on UWB and WLAN technologies.

5.2.1   UWB Ad Hoc Networks

When using TH-IR-UWB, u factor will be 1 since all nodes can use the medium at any time. In addition, g will reduce the interference power since spread-spectrum techniques are used in UWB technology.

5.2.1.1 Expected Interference Power for UWB

As seen in Figure 5.1, the highest number of interfering nodes will be around the center node n_0. Therefore, we will compute the total expected interference power $E[I]$ experienced at n_0. At node n_0 interference comes from all other nodes because we assume that all nodes in the

network can transmit simultaneously. The jth interfering ring contains 2 nodes at distance $j \cdot \Delta$ from $\mathbf{n_0}$. Therefore, using equation (5.1), the accumulative expected power level of interference coming from all interfering nodes in the network reduced by the processing gain g is then:

$$E[I] = \sum_{j=1}^{K} \frac{2 p_{tr} \cdot c (j \cdot \Delta)^{-\beta}}{g}$$
$$= \frac{2 p_{tr} \cdot c \cdot \Delta^{-\beta}}{g} \sum_{j=1}^{K} j^{-\beta} \tag{5.15}$$

where p_{tr} is the probability of packet transmission given by equation (5.8). If $K \to \infty$, equation (5.15) can be written as:

$$E[I] = \frac{2 p_{tr} \cdot c \cdot \Delta^{-\beta}}{g} \zeta(\beta) \tag{5.16}$$

where $\zeta(\beta) = \sum_{j=1}^{\infty} j^{-\beta}$ is the *Riemann-Zeta* function [1]. In wireless communications, β is always greater than 1. Hence, $\zeta(\beta)$ is a convergence series and upper bounded by [18]:

$$\sum_{j=1}^{\infty} j^{-\beta} \leq \left(1 + \int_{1}^{\infty} \frac{1}{x^{\beta}} \cdot dx = \frac{\beta}{\beta - 1} \right) \tag{5.17}$$

Therefore, $E[I]$ in TH-IR-UWB networks with line topology is upper bounded by:

$$E[I] < \frac{2 p_{tr} \cdot c \cdot \Delta^{-\beta} \cdot \beta}{g(\beta - 1)} \tag{5.18}$$

Notice that equality is removed from equation (5.18) because $k \ll \infty$ in practical networks.

5.2.1.2 Expected Signal Power for UWB

The useful signal will come from one of the nodes that has a direct link with node $\mathbf{n_0}$, i.e., from a node inside the coverage area of $\mathbf{n_0}$. As seen in Figure 5.1, there are 2α nodes within this area in addition to $\mathbf{n_0}$. For $j \leq \alpha$, the jth ring contains 2 nodes at distance $j \cdot \Delta$ from $\mathbf{n_0}$. The probability that the useful signal originated from the jth ring is then $2/2\alpha = 1/\alpha$. Therefore, using equation (5.1), the expected power level of the useful signal taking into account all possible rings is given by:

$$E[S] = \sum_{j=1}^{\alpha} \frac{c(j \cdot \Delta)^{-\beta}}{\alpha}$$

$$= \frac{c \cdot \Delta^{-\beta}}{\alpha} \sum_{j=1}^{\alpha} j^{-\beta}$$

(5.19)

5.2.1.3 Expected Channel Capacity for UWB

Using equations (5.15) and (5.19), $E[S/I]$ is given by:

$$E[S/I] = \frac{E[S]}{E[I]} = \frac{g \sum_{j=1}^{\alpha} j^{-\beta}}{2\alpha \cdot p_{tr} \sum_{j=1}^{K} j^{-\beta}}$$

(5.20)

Substituting $E[S/I]$ given by equation (5.20) in equation (5.14), the expected capacity of a link between two nodes inside the coverage area of each other is given by:

$$C = W \cdot log_2 \left(1 + \frac{g \sum_{j=1}^{\alpha} j^{-\beta}}{2\alpha \cdot p_{tr} \sum_{j=1}^{K} j^{-\beta}} \right)$$

(5.21)

where:

$$W = r \quad ;$$
$$p_{tr} = 1 - exp(-\lambda \cdot E[h]) \quad ;$$
$$\lambda = \frac{r_b}{r} \quad ;$$
$$E[h] = \frac{N_r + 1}{3} + 2\left(1 - \frac{N_r}{N}\right);$$
$$N_r = 1 + 2\left\lfloor \frac{K}{\alpha} \right\rfloor;$$
$$K = \frac{N-1}{2}; \quad N \text{ is always odd.}$$

The capacity given by equation (5.21) represents $r_{o,max}$ per node in line topology ad hoc networks using TH-IR-UWB multiple access scheme. Therefore, the maximum allowed basic throughput per node $r_{b,max}$ can be determined by equation (5.11) .

We use equations (5.10) and (5.21) to plot the output throughput per node r_o showing the saturation points due to channel capacity C limit and transmission bit rate r limit. For

example, 1Mb/s is a typical value of r as proposed by IEEE 802.15.4a group [26]. For indoor industrial application, we can choose β to be 2.15 for Non Line of Sight (NLOS) wireless communications, according to the final report of UWB channel model provided by IEEE 802.15.4a [39]. Let r_b be 50Kb/s. Using these values, r_o and C are plotted as functions of number of nodes N in the network. The plots are shown in Figure 5.3 for different values of processing gain g and density of nodes represented by α. Notice that number of nodes considered in the figures is very common in the production line network scenario described in Chapter 4. In this scenario, source-destination pairs are mainly 3 hops apart and these pairs along the line interfere with each other. When α=10, one should remember that number of relay nodes N_r is about 10 times less than number of nodes N in the network.
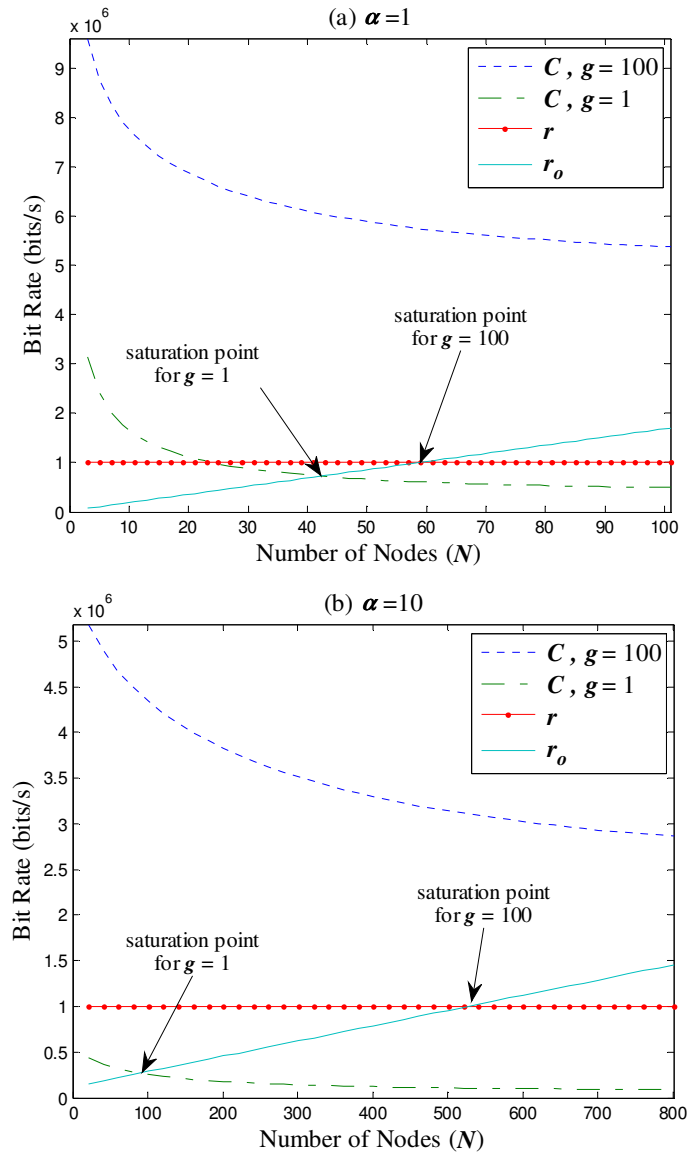

Figure 5.3: r_o Limits in UWB Ad Hoc Networks.

As shown in Figure 5.3(a), the value of g affects significantly C. When g=1, this denotes that there is no spreading of the signal power. Thus, there is no reduction of the interference level. Consequently, C sinks to values lower than r. As a result, r_o is limited basically by channel

capacity. However, when $g=100$, C becomes very large. In this case, r_o is limited by the transmission bit rate r. In UWB ad hoc networks g is very large and it could be around 5000. Therefore, as expected, UWB ad hoc networks with line topology have very large channel capacity. As a result, the transmission bit rate is the main limit of output throughput per node r_o in such networks.

The density of nodes in the line topology can be increased by increasing the value of α. If the nodes density increases, the interference level will increase as well. This will result in lower C as shown in Figure 5.3(b). However, with the large value of g, UWB ad hoc networks with line topology still have very large channel capacity as indicated in Figure 5.3(b), and the transmission bit rate is still the main limit of output throughput per node r_o in such networks.

5.2.2 WLAN Ad Hoc Networks

If the basic form of CSMA/CA protocol is considered, the calculation of the channel capacity using equation (5.14) will be different. Assuming that transmission range equals to interference range, among $(1+2\alpha)$ nodes inside the coverage area of any node in the line topology, e.g., $\mathbf{n_0}$ in Figure 5.1, only one node can transmit at a time. In this case, $\mathbf{u}$ factor equals to the reciprocal of $(1+2\alpha)$. Hence, C has to be divided by $(1+2\alpha)$ to include $\mathbf{u}$ factor. The channel capacity is then:

$$C = \frac{W}{1+2\alpha} log_2 \left(1 + E[S/I]\right) \tag{5.22}$$

The calculation of $E[S]$ at $\mathbf{n_0}$ is the same as in UWB ad hoc networks and it is given by equation (5.19). However, the calculation of $E[I]$ is different. Let we calculate the total expected interference power $E[I]$ experienced at $\mathbf{n_0}$. Since only one node is allowed to transmit inside the coverage area of $\mathbf{n_0}$, the first interfering ring is located just outside this coverage area, i.e., at distance $(\alpha+1)\Delta$ from $\mathbf{n_0}$. The next interfering ring is located just outside the coverage area of the nodes on the previous interfering ring at distance $(\alpha+1)\Delta$ from it. For $j \leq \lfloor K/(\alpha+1) \rfloor$, the jth interfering ring contains 2 nodes at distance $j(\alpha+1)\Delta$ from $\mathbf{n_0}$. Thus, using equation (5.1), the accumulative expected power level of interference coming from all interfering nodes in the network is given by:

$$E[I] = \sum_{j=1}^{\left\lfloor \frac{K}{\alpha+1} \right\rfloor} \frac{2 p_{tr} \cdot c \left(j(\alpha+1)\Delta\right)^{-\beta}}{g}$$

$$= \frac{2 p_{tr} \cdot c \cdot \Delta^{-\beta} (\alpha+1)^{-\beta}}{g} \sum_{j=1}^{\left\lfloor \frac{K}{\alpha+1} \right\rfloor} j^{-\beta} \tag{5.23}$$

where p_{tr} is given by (5.8) and g is the processing gain since spread-spectrum techniques are also used in WLAN technology. Therefore, $E[I]$ for WLAN ad hoc networks with line topology is upper bounded by:

$$E[I] < \frac{2p_{tr} \cdot c \cdot \Delta^{-\beta} \cdot \beta}{g(\beta-1)}(\alpha+1)^{-\beta} \tag{5.24}$$

Notice that equality is removed from equation (5.24) because k << ∞ in practical networks. Using equations (5.19) and (5.23), $E[S/I]$ is given by:

$$E[S/I] = \frac{g(\alpha+1)^{\beta} \sum_{j=1}^{\alpha} j^{-\beta}}{2\alpha \cdot p_{tr} \sum_{j=1}^{\left\lfloor \frac{K}{\alpha+1} \right\rfloor} j^{-\beta}} \tag{5.25}$$

Substituting $E[S/I]$ given by equation (5.25) in equation (5.22), the expected capacity of a direct link between two nodes is given by:

$$C = \frac{W}{1+2\alpha} \cdot log_2 \left(1 + \frac{g(\alpha+1)^{\beta} \sum_{j=1}^{\alpha} j^{-\beta}}{2\alpha \cdot p_{tr} \sum_{j=1}^{\left\lfloor \frac{K}{\alpha+1} \right\rfloor} j^{-\beta}} \right) \tag{5.26}$$

The capacity given by equation (5.26) represents $r_{o,max}$ per node in WLAN ad hoc networks with line topology and CSMA/CA multiple access scheme. Therefore, the maximum allowed basic throughput per node $r_{b,max}$ can be determined by (5.11).

We use equations (5.10) and (5.26) to plot the output throughput per node r_o showing the saturation points due to channel capacity C limit and transmission bit rate r limit. For example, 1Mb/s is a typical value of r as proposed by IEEE 802.11 standard [59]. For indoor industrial application, we can choose β to be 2.15 for NLOS wireless communications. Let r_b be 50Kb/s. Using these values, r_o and C are plotted as functions of number of nodes N in the network. The plots are shown in Figure 5.4 for different values of processing gain g and nodes density represented by α.

Comparing Figure 5.4(a) with Figure 5.3(a), we can see that at low density of nodes, the saturation points of r_o in WLAN ad hoc networks occur due to the same limits as in UWB ad hoc networks but at a different point for channel capacity limit with lower value. However, when the density of nodes increases, C decreases rapidly and becomes lower than the transmission bit rate r even for large values of g. In practice, g in WLAN is much lower than 100. A typical value of g is 11 as proposed by IEEE 802.11 standard [59]. Therefore, WLAN ad hoc networks with line topology have very low channel capacity as indicated in Figure 5.4(b) and channel capacity is the main limit of output throughput per node r_o in such networks. In other words, by comparing Figure 5.3(b) with Figure 5.4(b), we can see clearly that UWB technology outperforms WLAN technology in ad hoc networks with line topology. This explains why there is a big difference in the achieved normalized throughput in the

production line scenario using UWB and WLAN technologies. This is further verified in the next subsection.
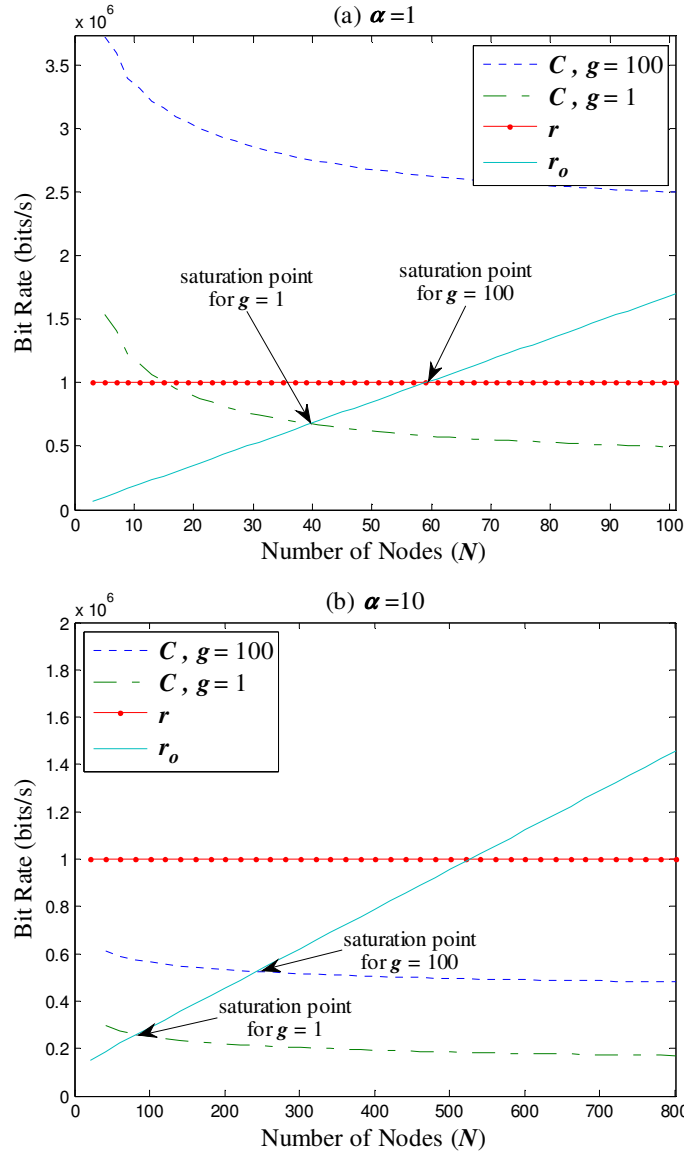
Figure 5.4: r_o Limits in WLAN Ad Hoc Networks.

5.3 Model Verification

5.3.1 Simulation Results

The line topology shown in Figure 5.5 was simulated using ns-2 [45] version ns-allinone-2.29.3 running under SUSE Linux 10.1 operating system. WLAN technology operating with IEEE 802.11 standard [59] is implemented in the above ns-2 version. However, UWB technology is not implemented so far. Thus, the code version ns-2.29-uwb-0.10.0 was used [63] for UWB technology. The simulation time was 100s. To achieve a reasonable confidence interval, each simulation experiment was repeated 25 times and their average has been used. The 99% confidence intervals for the simulation results are included in the plots. Our

simulation software is freely available [56]. Also, our institute IKT will be provided with a copy of the simulation software on a CD.

We simulated the line topology with 5 relay rings as shown in Figure 5.5, to resemble the production line shown in Figure 4.2 with one traffic flow. Transmission range of all nodes R is always fixed, e.g., 10m. Number of nodes in the topology depends on the value of α and K. For example, α is 1 and K is 5 in Figure 5.5.The value of α is varied to take the values 1, 2 and 5; for K=5, 10 and 25 respectively. Thus, the ratio K/α is always 5, i.e., 5 relay rings. By increasing the value of α, we increase node density in the network by decreasing the distance between nodes Δ as shown in Figure 5.5. For each of (α, K) pair value, the basic throughput per node r_b is varied to measure the saturation point of the simulated output throughput per node $r_{o,sim}$. The results are shown in Figure 5.6 and Figure 5.7 for WLAN and UWB technologies respectively. In these figures, the channel capacity C is also plotted as a function of the basic throughput per node r_b.
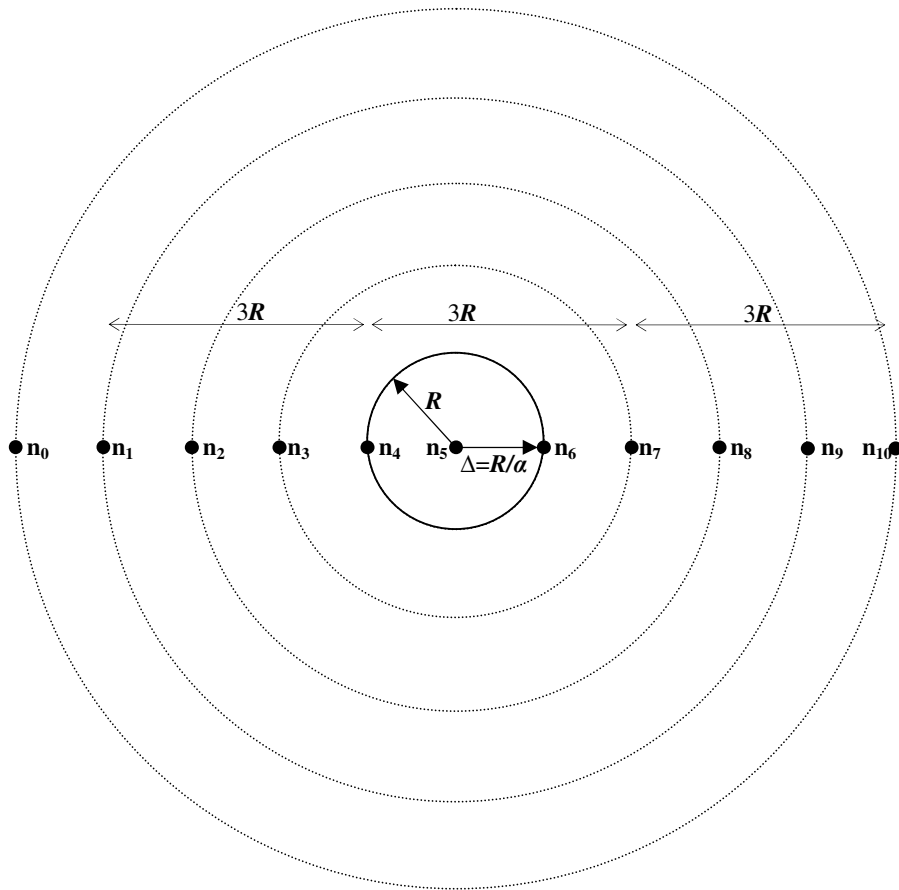
Figure 5.5: Line Topology with 5 Relay Rings
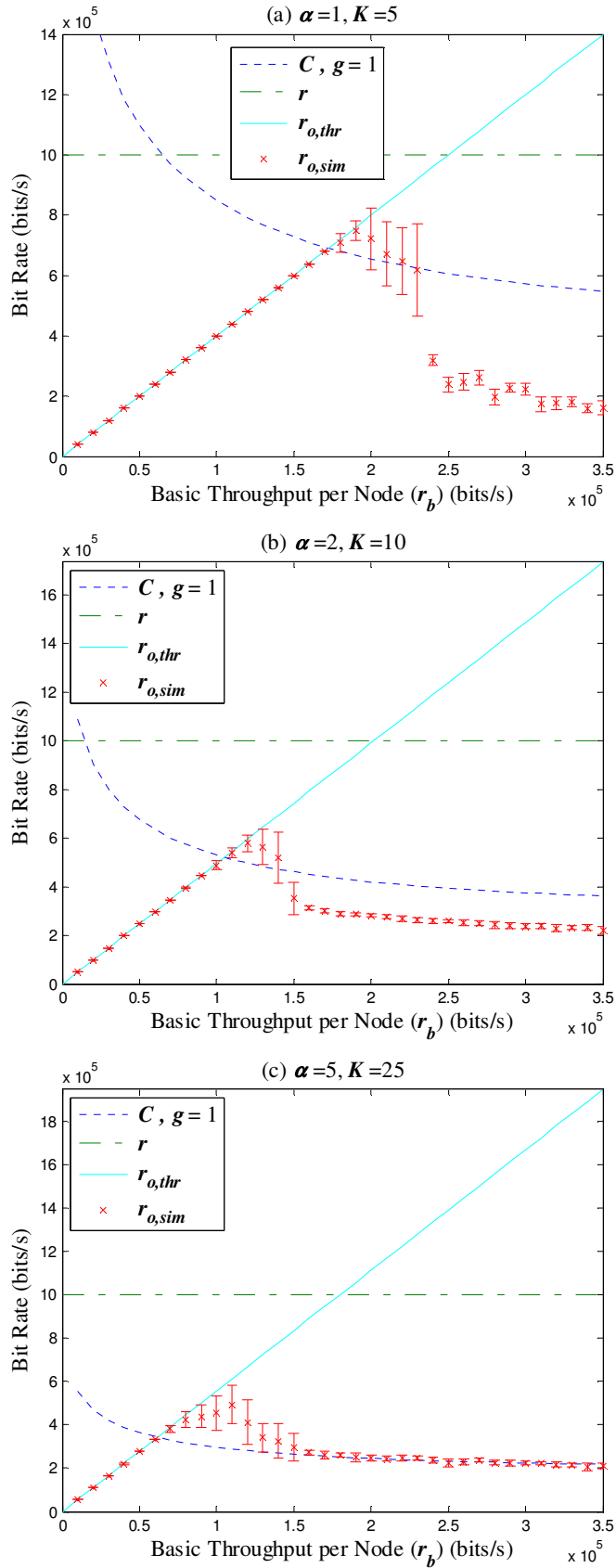
Figure 5.6: Simulated r_o using WLAN Technology.

In Figure 5.6, the theoretical and simulated r_o are plotted versus r_b using WLAN technology. $r_{o,thr}$ is plotted using equation (5.10). Also, C is plotted using equation (5.26). In these plots, r is 1Mb/s and β is 2.15. With these settings, $r_{o,thr}$ and $r_{o,sim}$ are plotted for α=1, 2 and 5; while K=5, 10 and 25 respectively. As shown in Figure 5.6, $r_{o,sim}$ increases as r_b increases until the saturation point of channel capacity is reached. After this saturation point, $r_{o,sim}$ starts to sink and it is then limited by channel capacity. This is true for the three cases, i.e., for α=1, 2 and 5. It is noticed that the simulated saturation point is a little bit higher than the theoretical value. This is because re-transmissions due to packet loss and collisions are not included in the mathematical model, but it is included in the simulation and this is a source of error. However, this will mainly affect packet transmission probability p_{tr} at low r_b. Including re-transmissions will increase traffic in the network, and hence, p_{tr} will increase. But as r_b becomes large, p_{tr} reaches its upper bound value which is 1 and re-transmissions will not affect our model anymore. Therefore, for large r_b, we expect that $r_{o,sim}$ will converge to the same value as C especially for large values of α. This behavior is noticed in $r_{o,sim}$ as shown in Figure 5.6.
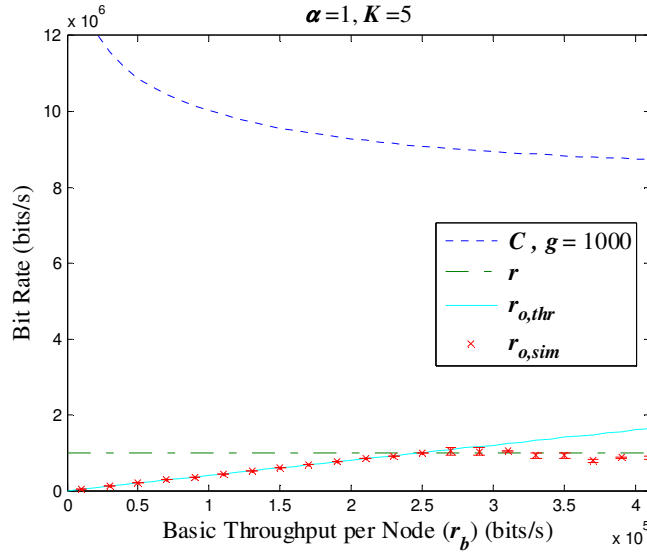
Figure 5.7: Simulated r_o using UWB Technology.

In Figure 5.7, the theoretical and simulated r_o are plotted versus r_b using UWB technology. $r_{o,thr}$ is plotted using equation (5.10). In this plot, r is 1Mb/s and β is 2.15. With these settings, $r_{o,thr}$ and $r_{o,sim}$ are plotted for α=1; while K=5. As shown in Figure 5.7, $r_{o,sim}$ increases as r_b increases until the saturation point of transmission bit rate r is reached. After this saturation point, $r_{o,sim}$ does not increase anymore and it is then limited by the transmission bit rate r. Thus, the saturation point in UWB is determined by the transmission bit rate r because it is much smaller than the channel capacity C as shown in Figure 5.7.

The simulation results shown in Figure 5.6 and Figure 5.7 verify our mathematical model. Also, it is worth noting that our finding regarding the maximum basic throughput per node $r_{b,max}$ given in equation (5.11) agrees with results found in literature. For example, in [23], $r_{b,max}$ (or the throughput capacity per node as called by the authors) is found to be in the form $O\left(1/\sqrt{N}\right)$. In [24], the author shows that $E[h]$ of the network topology used in [23] is $O\left(\sqrt{N}\right)$. Therefore, $r_{b,max}$ for wireless networks with topology used in [23] according to

51

equation (5.11) is $O\!\left(1/\sqrt{N}\right)$. Furthermore, our analytical calculations regarding r_o comply with (or can explain) the simulation results obtained in [29] which uses the line topology.

5.3.2 Effect of Propagation Model

In our simulation experiments in section 4.3, the basic throughput per node r_b is very low and therefore the output throughput per node r_o is in the range of few Kbps even if packet retransmission, duplication and routing overhead is considered. At this range, neither the transmission bit rate limit nor the channel capacity limit found in this Chapter is reached definitely. Therefore, according to our mathematical model developed in this Chapter, we expect to obtain a normalized throughput NTh of 100%. This will be true, if the power law model is used. But in these simulation experiments, the shadowing model is used. Therefore, NTh does not reach 100% in multi-hop communications and stays at low levels, especially for WLAN technology, as shown in Figure 4.3 for example.

To see the effect of the propagation model on the channel capacity, and hence on NTh, we repeated the multi-hop investigation in section 4.3.1 using power low model. We repeated the simulation experiments for WLAN technology since it has a much lower throughput than UWB technology. The production line with one data traffic flow shown in Figure 4.2 was used. The network consists of two fixed nodes and mobile nodes moving from one side to the other. The distance between fixed nodes is varied to take the values 10m, 20m, and 30m. For each of these values, the distance between mobile nodes is varied from 1m to 30m. Data traffic consists of only one flow between the two fixed nodes with the basic data rate of 0.27Kb/s and using TCP connections. The results are shown in Figure 5.8.

When the distance between the two fixed nodes is 10m, the communication between them is done mainly in one hop (direct connection link). Therefore, there is no multi-hop communications and NTh is 100% for both propagation models as shown in Figure 5.8(a).

When the distance between the two fixed nodes is 20m, the communication between them is done mainly in two hops, and thus, the multi-hop effect on NTh obviously appears as shown in Figure 5.8(b). As the distance between mobile nodes becomes larger than the transmission range, there are insufficient nodes for multi-hop communications. Accordingly, NTh decreases in this case for both propagation models. On the other hand, as the distance between mobile nodes becomes smaller than the transmission range, there are extra nodes than what are needed for multi-hop communications. The effect of these extra nodes appears in WLAN that uses shadowing model only, in which NTh decreases as distance between mobile nodes decreases. In case of power law model, NTh stays at 100%.

When the distance between the two fixed nodes is increased to 30m, the communication between them is done mainly in three hops. Figure 5.8(c) shows clearly that fading phenomena represented by shadowing model will significantly reduce the channel capacity in multi-hop communications.
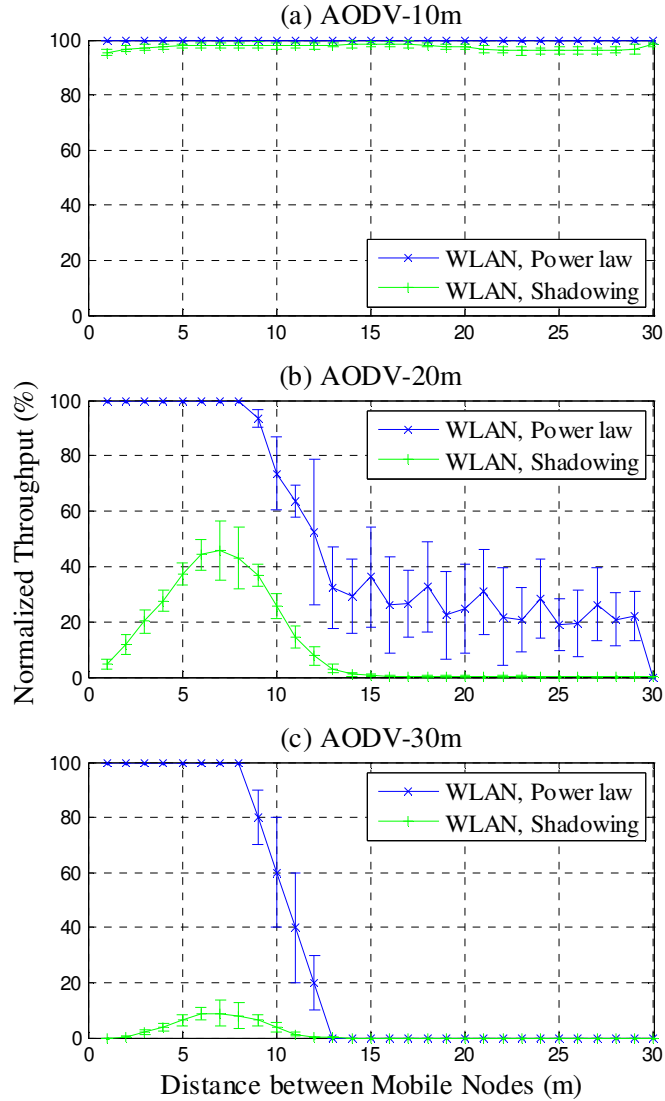
Figure 5.8: Effect of Propagation Model on Normalized Throughput.

5.4 Model Restrictions

In our model, the channel capacity is calculated for the networks with line topology in which the nodes are distributed uniformly. Hence, this calculation will not be valid if the uniform distribution is disrupted. Also, our model assumes that the nodes are fixed in their locations. However, the calculation of the channel capacity remains valid as long as uniform distribution of nodes is not affected by moving nodes. In spite of this restriction, our model is applicable and can be used in the production line application described in Chapter 4, in which the network consists of moving nodes that are uniformly distributed along a line topology.

In addition, re-transmissions due to packet loss and collisions are not included in traffic. This will mainly affect packet transmission probability p_{tr}. However, regardless the exact expression of p_{tr}, we can explain the effect of it on channel capacity computation. Including re-transmissions will increase traffic in the network, and hence, p_{tr} will increase. With higher p_{tr}, the channel capacity will decay more rapidly but it will always converge to the same value

since $p_{tr} \leq 1$. This behavior is verified using equations (5.21) and (5.26). In this context, our model still gives a lower bound for channel capacity when $p_{tr}=1$ in case of full network load or excessive data traffic.

Finally, we assume that the pathloss power law model for radio propagation is used. This assumption is the ideal case but it is not practical under fading conditions. Therefore, a more realistic pathloss model should be considered, e.g., a pathloss shadowing model. This is the main limitation of our model as shown in the previous section.

5.5 Summary and Conclusions

In this chapter closed-form formulas are found for the channel capacity of ad hoc networks with line topology based on UWB and WLAN technologies. The starting point for the computation is the Shannon channel capacity equation. However, an additional restriction on channel capacity is imposed by the multiple access scheme used in the network. Furthermore, the used multiple access scheme and spread-spectrum technique affect the calculation of interference level.

It is found that the capacity of ad hoc network with line topology depends on number of nodes, density of nodes, processing gain, hop-count distribution, and data traffic. It is also found that interference level is upper bounded for large network size. Therefore, the capacity is lower bounded. In case of ad hoc networks with line topology based on UWB technology, the upper bound of interference depends on probability of packet transmission, average power of transmission, distance between nodes, pathloss exponent, and processing gain as it can be seen from equation (5.18). Thus, even for excessive data traffic, the interference will be still upper bounded since the probability of packet transmission will not exceed 1. In case of WLAN technology, and assuming the same data traffic, power transmission, distance between nodes, and processing gain as in UWB technology, the interference upper bound expressed in equation (5.24) is reduced by a factor of $(\alpha+1)^{-\beta}$ which is always less than 1 since α and β are always greater than or equal to 1.

However, the channel capacity of ad hoc networks with line topology based on WLAN technology is much lower than that based on UWB technology for the same scenario especially for a high density of nodes. This is due to the fact that the channel inside a certain coverage area in WLAN is shared by many nodes and only one node among them can access the channel at a time. In contrast, with UWB technology the channel can be accessed by all nodes simultaneously. In addition, UWB technology has a much larger processing gain. As a result, the output throughput per node r_o is limited mainly by the transmission bit rate r in case of UWB technology. On the other hand, r_o is limited mainly by channel capacity in case of WLAN technology.

Our model is derived for the line topology configuration since it can be used in the production line in a factory. Following a similar systematic model, the channel capacity can be found for other topology configurations as well.

One more conclusion is that the channel capacity is maximized when routing is done using the energy conservation method, i.e., when $\alpha=1$. This method will ensure that the minimum

number of nodes inside the coverage area of a node is used. Therefore, the interference level will be minimized.

Finally, this work presents a simple systematic model by which the factors affecting channel capacity can be easily controlled to understand their role in channel capacity computations. The main restriction of this model is the pathloss power law model used for radio propagation.

6 AD HOC ON-DEMAND MULTIPATH SOURCE ROUTING

In this chapter, we describe in details our approach to design an enhanced routing protocol suitable for our network scenario. Then the performance of the new routing protocol is investigated and compared to the performance of AODV, DSR and OLSR. Our proposed routing protocol was implemented in ns-2 simulator to be used in the performance evaluation.

6.1 Overview

In section 4.4, we described briefly two approaches to design efficient routing protocol for our network scenario which is a production line in a factory. The first approach is based on modifications of existing routing protocols, while the second approach is based on a new routing protocol. We chose to focus on the first approach and leave the second approach for future work.

The idea behind the first approach is that each routing protocol studied in chapter 4 has some routing mechanisms that will lead to better routing performance if they are combined in one routing protocol. These mechanisms are as following:

- timer to delete unused routes (AODV mechanism)
- multipath routing (DSR mechanism)
- source routing (DSR mechanism)
- control number of forwarding nodes and paths (OLSR mechanism)

We found that AODV outperforms DSR and OLSR especially in large network size. Therefore, the idea was to start with AODV and modify its implementation code in ns-2 to include the mechanisms used in the other two protocols. However, the authors of [33] propose multipath extensions to AODV and the resulting protocol is called Ad Hoc On-Demand Multipath Distance Vector (AOMDV). Therefore, we chose to modify the implementation code of AOMDV. Now, the first mechanism is already implemented in AOMDV since it is an extension of AODV. The second mechanism is also implemented in AOMDV but it should be modified in order to work properly with the last two mechanisms that are not implanted in AOMDV. Combining these four mechanisms in one routing protocol will result in a new robust protocol suitable for our network scenario. We will call this protocol Ad Hoc On-Demand Multipath Source Routing (AOMSR) protocol. The main objective of AOMSR is to reduce the time of route discovery and maintenance in order to achieve better performance.

Before describing AOMSR, it is important to give an overview on AOMDV. The main difference between AOMDV and AODV is in the number of route paths found in each route discovery. In AODV, for each RREQ initiated by a source node, only one RREP is accepted to set a new route entry or replace an older entry for a certain destination. This means that the routing tables in AODV contain only one route entry per destination. On the other hand, AOMDV accepts many RREPs for each RREQ. Therefore, route tables in AOMDV maintain multiple route entries for each destination. By this way, nodes in AOMDV are provided with alternate routes. Therefore, if a route breaks, a node can find another route without initiating a new RREQ. As a result, this will reduce route discovery frequency in AOMDV [43].

However, maintaining multiple routes per destination may lead to loop problem, especially in protocols by which a node only keeps information of the next hop and distance from destination via the next hop. This limited one hop information causes loop problem [33]. The core of AOMDV protocol lies in ensuring that multiple routes discovered and updates are loop-free. Since a node keeps only one hop information, AOMDV ensures loop-free using relatively complicated rules that limit the usefulness of multipath mechanism.

In AOMSR, we solve the loop problem using source routing mechanism. In AOMSR, every node maintains complete path information for each route. Therefore, ensuring loop-free becomes straightforward. A path is loop-free if each node appears only once in the path. Obviously, source routing will increase routing overhead since packet headers should contain complete path information at each node. However, in our scenario, the communications between source-destination nodes is done mainly in 3 hops as described in Chapter 4. Besides, line topology using UWB technology has a high channel capacity as shown in Chapter 5. Therefore, we expect that routing overhead added by source routing will not be a limiting factor in our network scenario.

Another reason for using source routing mechanism is that it will facilitate controlling number of forwarding nodes and paths in the network. This is achieved using the disjoint paths concept [33]. Disjoint paths are an efficient subset of alternate paths taken from a larger set of all paths between any source-destination pair. The probability of a simultaneous failure of all disjoint paths between any source-destination pair is very small. There are two kinds of disjoint paths: link disjoint and node disjoint. Link disjoint paths have no common links between a source-destination pair, while node disjoint paths have no common nodes. Since a node keeps only one hop information in AOMDV, selecting disjoint paths is done using relatively complicated inefficient rules. On the other hand, selecting disjoint paths in AOMSR is straightforward and more robust since each node maintains complete path information for each route. A path is disjoint if it has no common link or node with another path. Disjoint paths help in controlling number of forwarding nodes and paths in the network, and hence, reducing some unwanted overhead in the network such packet duplication.

6.2   AOMSR Protocol Description

Since AOMSR is an extension to AOMDV which is itself an extension to AODV, we will explain in this section the main enhancements and differences between AOMSR in one side and AOMDV and AODV on the other side.

6.2.1   Routing Table Entry

The differences in route table entry structure for AOMSR, AODV and AOMDV are shown in Figure 6.1. AODV maintains only one route path per destination and it consists of destination address, sequence number of the route, hop count towards the destination, next hop node towards destination and time-to-live for this route. AOMDV adds new fields in order to maintain multiple paths per destination. Route entry of AOMDV consists of destination address, sequence number of the route, advertised hop count and path list. The path list contains information for each path and it consists of next hop node towards the destination, last hop node before the destination, hop count towards the destination and time-to-live for this route path. Therefore, route entry size of AOMDV is not constant since it contains a list

of route paths for each destination. Furthermore, AOMDV introduces two new fields: advertised hop count and last hop. Advertised hop count is used to avoid loops that may arise because of the multiple paths and it is set to the hop count of longest path in the list. Last hop is used to choose disjoint paths.

In AOMSR, the route entry consists of destination address, sequence number of the route and path list. The path list contains information for each path and it consists of the complete path information of all nodes from current node to the destination node and time-to-live for this route path. Therefore, like AOMDV, route entry size of AOMSR is not constant also. However, unlike AOMDV, hop count information is not needed since the complete path information is available in the path list.

destination	sequence number	hop count	next hop	timeout

(a) AODV

destination	sequence number	advertised hop count	path list			
			next hop1 next hop2 . .	last hop1 last hop2 . .	hop count1 hop count2 . .	timeout1 timeout2 . .

(b) AOMDV

destination	sequence number	path list	
		nodes along path1 nodes along path2 . .	timeout1 timeout2 .

(c) AOMSR

Figure 6.1: Structure of Routing Table Entry for AODV, AOMDV and AOMSR.

6.2.2   Route Update Mechanism

In AOMSR, AODV and AODV, when a node needs to send data packets to a destination with no valid route, a route discovery procedure is initiated by flooding RREQ in the network and waiting RREP from the destination or an intermediate node that has a valid route to the destination. During this process, nodes update their routing tables making use of RREQ and RREP messages. For comparison reasons, simplified route update algorithms for the three routing protocols are listed in Table 6.1. In AODV, a node updates its routing table entry for a certain destination if one of two conditions is satisfied. Either if the route information contained in RREQ or RREP has a higher sequence number (i.e., more recent) than that of table route entry, or if the route information contained in RREQ or RREP has the same sequence number as that in table route entry but with shorter path (smaller hop count). These two conditions are checked in the line 1 in Table 6.1(a).

In AOMSR, the first condition is checked in line 1 in Table 6.1(c), and if it is true all old paths in the route entry will be deleted and replace by the new path. The second condition is modified and checked in separately in another line in order to accept multiple paths for the same destination as it is seen in line 5 Table 6.1(c). Here, if the route information contained in RREQ or RREP has the same sequence number as that in table route entry but with a different

59

loop-free path, the new path will be added to path list if it is a disjoint path (line 7 in Table 6.1(c)). A path is loop-free if each node appears only once in the path, and it is a disjoint path if it has no common link with another path in the list.

Table 6.1: Route Update Algorithms for AODV, AOMDV and AOMSR.

1: **if** (seq_num in route entry < seq_num in RREQ or RREP) or ((seq_num in route entry =
    seq_num in RREQ or RREP) and (hop_count in route entry > hop_count in RREQ or
    RREP))
2: **Begin**
3:   replace route entry with the new path
4: **End**

(a) AODV

01: **if** (seq_num in route entry < seq_num in RREQ or RREP)
02: **Begin**
03:   delete all old paths in the route entry and add the new path for the destination
04: **End**
05: **elseif** ((seq_num in route entry = seq_num in RREQ or RREP) and (adv_hop_count in
    route entry > adv_hop_count in RREQ or RREP))
06: **Begin**
07:   **if** (the new path is disjoint [***using next and last hop information***])
08:   **Begin**
09:     add the new path to route entry
10:   **End**
11: **End**

(b) AOMDV

01: **if** (seq_num in route entry < seq_num in RREQ or RREP)
02: **Begin**
03:   delete all old paths in the route entry and add the new path for the destination
04: **End**
05: **elseif** (seq_num in route entry = seq_num in RREQ or RREP) and (path is loop-free
    and it is not already exist in the path list)
06: **Begin**
07:   **if** (the new path is disjoint [***using nodes along path information***])
08:   **Begin**
09:     add the new path to route entry
10:   **End**
11: **End**

(c) AOMSR

The route update algorithm used in AOMSR is a modified version of that used in AOMDV. The differences between them appear in lines 5 and 7 as shown in Table 6.1(b) and Table 6.1(c). Line 5 checks for loop-free path, while line 7 checks for disjoint path. These two tests are straightforward in case of AOMSR since all route information is found in the packet header. In case of AOMDV, these tests are much more complicated. AOMDV uses hop count and advertised hop count for loop-free test, while it uses next and last hop for disjoint test. For

more information on AOMDV we refer the reader to [33] because details of AOMDV are beyond the scope of this thesis.

6.2.3 Route Maintenance Mechanism

AOMSR uses the same procedure used in AOMDV for route maintenance. A path is used until it expires or breaks. Link breaks are confirmed by RERR messages. If a path becomes unavailable, then the next path in the list is used. When there are no more paths in the list, then a maintenance procedure using RERR packets is initiated in order to initiate a route discovery procedure. This is the same maintenance procedure used in AODV as described in Chapter 3.

6.3 Performance Evaluation

In this section, we investigate the performance of AOMSR and compare it to the performance of AODV, DSR and OLSR in the production line scenario defined in Chapter 4. In the following subsections we discuss the simulation results.

6.3.1 Data Rate Investigation

The production line with one data traffic flow shown in Figure 4.5 was used to investigate the data rate effect on the performance of AOMSR based on UWB technology. The network consists of two fixed nodes and mobile nodes moving from one side to the other. The mobile nodes are uniformly distributed. The distance between the two fixed nodes is set permanently to 30m, while the distance between mobile nodes is varied from 1m to 30m with 1m step increment. Therefore, number of mobile nodes in the network is variable and it is between 3 and 90 nodes depending on the distance between mobile nodes. Length of the production line is 90m. Data rate of the data traffic flow is varied by sending one data packet of size 1024 bytes from one fixed node to the other every 30s (0.27Kb/s), 10s (0.82Kb/s), and 5s (1.64Kb/s). The results are shown in Figure 6.2. Furthermore, data packets distribution ratios, with respect to the total useful data packets that should be transmitted, are shown in Figure 6.3 for AOMSR.

Again, we would like to remind the reader that in our discussion, we refer to the region where the distance between mobile nodes is smaller than the transmission range as the region of high node density. Also, we refer to the region where the distance between mobile nodes is larger than the transmission range as the region of low node density. Unless otherwise stated, we discuss the curves and results around the transmission range region of each routing protocol.

To simplify the discussion and to compare the performance of AOMSR with AODV, DSR and OLSR, Table 6.2 is constructed from Figure 6.2, Figure 4.6, Figure 4.7 and Figure 4.8. Therefore, we will focus in our discussion on Table 6.2 but we may refer the reader to Figure 6.2 and Figure 6.3 when they are needed. Table 6.2 shows the ratio of AOMSR performance parameters to that of AODV, DSR and OLSR as data rate is being increased. It is obvious that AOMSR achieves larger PDR and NTh than AODV and DSR. Moreover, as data rate increases, the enhancement ratio gets larger. For example, PDR of AOMSR at 0.27Kb/s is about 1.29 times PDR of AODV and about 2.31 times PDR of DSR, while it increases at 1.64Kbps to reach about 2.02 times PDR of AODV and about 5.57 times PDR of DSR. The same behavior is noticed for NTh.
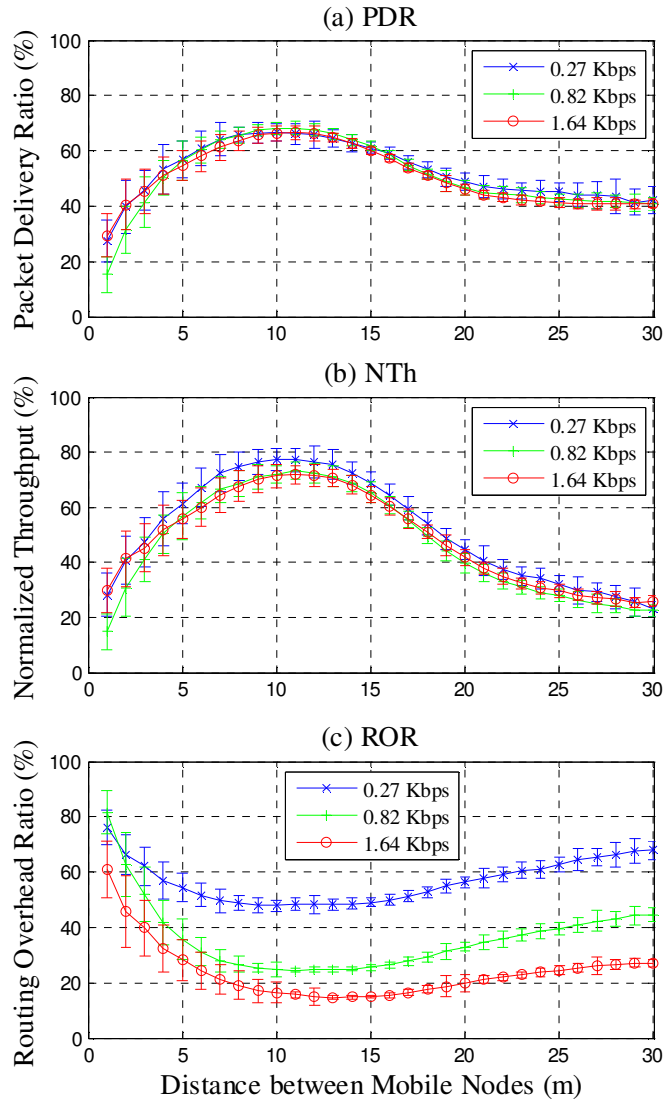
Figure 6.2: Data Rate Effect on AOMSR Performance.

Table 6.2: Ratio of AOMSR Performance Parameters in Data Rate Investigation

	Ratio of max. **PDR** of AOMSR to that of:			Ratio of max. **NTh** of AOMSR to that of:			Ratio of min. **ROR** of AOMSR to that of:		
	AODV	DSR	OLSR	AODV	DSR	OLSR	AODV	DSR	OLSR
0.27kb/s	1.29	2.31	1.24	0.98	1.40	1.93	3.00	1.02	0.64
0.82kb/s	1.58	4.00	1.19	1.24	1.83	1.24	1.92	0.64	0.62
1.64kb/s	2.02	5.57	1.12	1.90	2.48	1.08	1.25	0.51	0.67

Also, AOMSR achieves larger PDR and NTh than OLSR. However, as data rate increases, the enhancement ratio gets smaller. This is because PDR and NTh of AOMSR do not increase as data rate increase (see Figure 6.2) while they do increase in OLSR (see Figure 4.6 and Figure 4.7) due the proactive nature of OLSR as explained in section 4.3.2.

As shown in Table 6.2, AOMSR has a much higher ROR than AODV. For example, ROR of AOMSR at 0.27Kb/s is 3 times ROR of AODV. This result is expected since AOMSR uses source routing mechanism. However, as data rate increases, ROR of AOMSR gets closer to that of AODV as shown in Table 6.2, i.e., ROR of AOMSR at 1.64Kb/s is 1.25 times ROR of AODV. Therefore, we expect that AOMSR will outperform AODV in terms of ROR at high data rates. This is because AODV initiates more route discovery and maintenance procedures with higher data rate as discussed in section 4.3.2. Also, as data rate increases, AOMSR outperforms DSR in terms of ROR as it is seen in Table 6.2. In addition, ROR of AOMSR is lower than that of OLSR by a factor of almost 1/3 regardless of data rate.
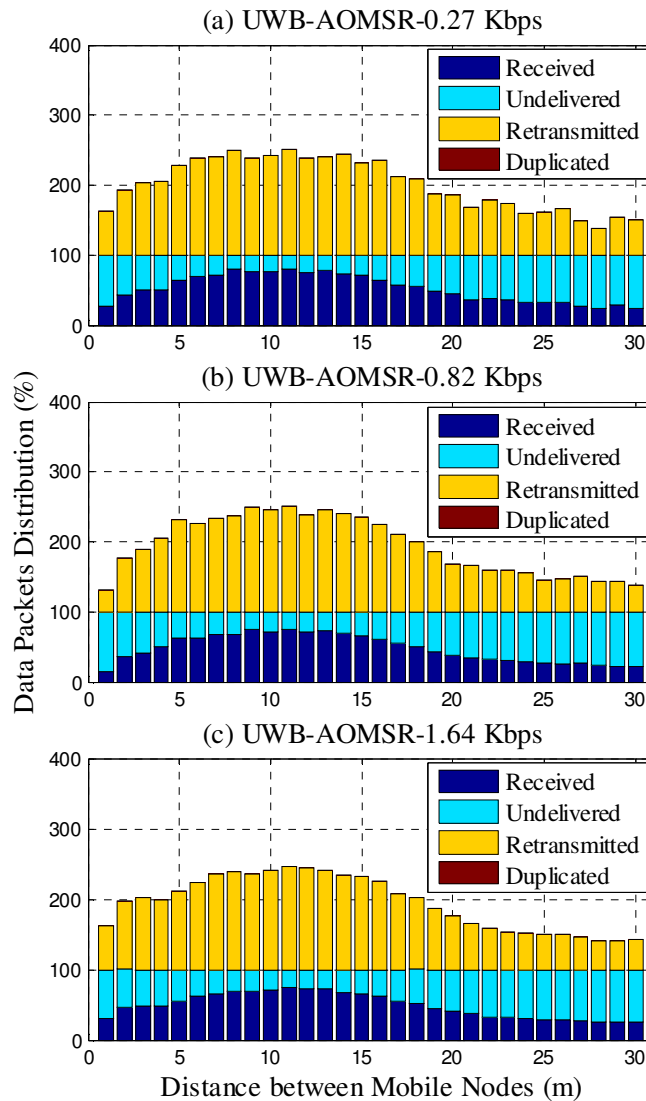

Figure 6.3: Data Rate Effect on AOMSR Data Packets Distribution.

From the previous discussion, it is shown that AOMSR has a better performance than AODV, DSR and OLSR in terms of PDR and NTh. It has also a better performance in term of ROR in case of DSR and OLSR. This is not true for AODV. However, since line topology using UWB technology has a high channel capacity as shown in Chapter 5, the increase in route overhead does not prevent AOMSR to achieve the same or better NTh than other protocols. For example, AOMSR achieves almost the same NTh as AODV at 0.27Kbps although ROR of AOMSR is 3 times that of AODV.

As a final observation, we can see in Figure 6.3 that AOMSR does not produce any data duplication. This is because routing tables in AOMSR are built using a more robust mechanism making use of disjoint paths. Therefore, AOMSR and OLSR share the same property of eliminating data packet duplications.

6.3.2   Scalability Investigation

Here we describe the scalability of AOMSR in the production line scenario using UWB technology. Production lines with one, three and eight data traffic flows were used. Figure 4.12 shows production lines with one and three data traffic flows. Number of fixed machines equals to the number of flows plus one. That is, the network consists of 2, 4 and 9 fixed nodes when there are one, three and eight data traffic flows respectively. The distance between fixed nodes is always 30m. There are also mobile nodes moving from one side to the other and they are uniformly distributed. The distance between mobile nodes is varied from 1m to 30m with 1m step increment. Number of mobile nodes is variable and it depends on the distance between mobile nodes and the length of the production line. Length of the production line equals to 30m multiplied by number of flows plus 30m before the first fixed machine and 30m after the last fixed machine. Therefore, number of mobile nodes is between 3 and 300. Data traffic consists of only one flow between each two successive fixed nodes with the basic data rate of 0.27Kb/s. The results are shown in Figure 6.4.

To simplify the discussion and to compare the scalability results of AOMSR with AODV, DSR and OLSR, Table 6.3 is constructed from Figure 6.4, Figure 4.13 and Figure 4.14. Table 6.3 shows the ratio of AOMSR performance parameters to that of AODV and OLSR as flow number is being increased. It is obvious that AOMSR outperforms OLSR in terms of NTh and ROR. Also, AOMSR outperforms AODV in terms of NTh especially for large number of flows, although AOMSR still have higher ROR than AODV.

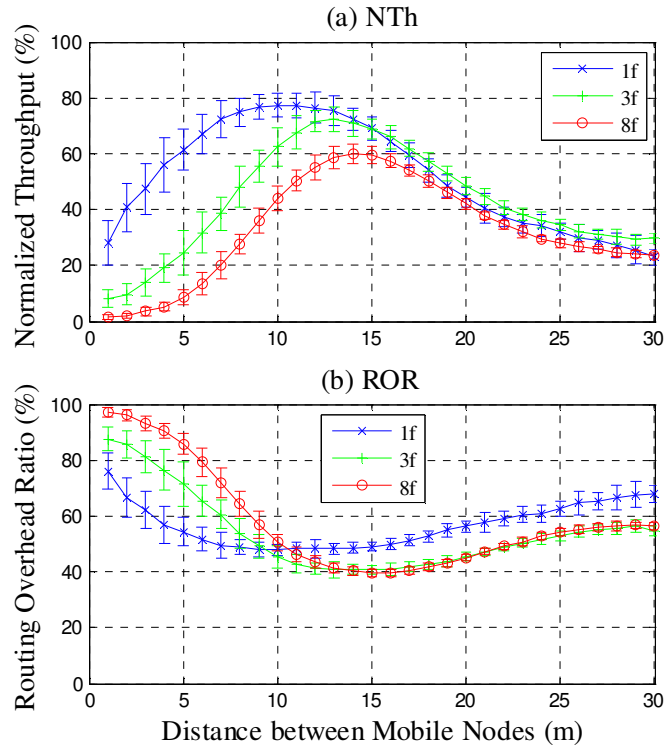Figure 6.4: Scalability Effect on AOMSR Performance.

Table 6.3: Ratio of AOMSR Performance Parameters in Scalability Investigation

	Ratio of max. **NTh** of AOMSR to that of:		Ratio of min. **ROR** of AOMSR to that of:	
	AODV	OLSR	AODV	OLSR
1Flow	0.98	1.93	3.00	0.64
3Flows	1.24	1.90	2.00	0.61
8Flows	1.30	2.10	2.00	0.61

6.4   Summary and Conclusions

This chapter describes how we design a new routing protocol suitable to our network scenario, and we call it Ad-Hoc On-Demand Multipath Source Routing (AOMSR) protocol. The idea was to combine many useful routing mechanisms from different routing protocols in one robust routing protocol. As a result, AOMSR uses routing tables, multiple route paths per destination, time threshold to delete inactive routes, and destination sequence number to determine the freshness of a route. In addition, it uses source routing mechanism to determine free-loop and disjoint paths in a robust simple way. Furthermore, AOMSR makes use of disjoint paths to control number of forwarding nodes in the network and to establish reliable route paths.

The combination of these routing mechanisms in one routing protocol makes from AOMSR an efficient routing protocol for our network scenario. As a result, it outperforms the other routing protocols considered in this study. Although AOMSR may increase routing overhead when compared to AODV since it uses source routing, but it still achieves better throughput. Moreover, AOMSR prevents data packet duplications. The main feature that makes AOMSR suitable to our network scenario is that it reduces time of route establishment (route discovery and maintenance) even if this may increase routing overhead to a certain extent.

7 SUMMARY, CONCLUSIONS AND FUTURE WORK

Wireless technologies are foreseen as the predominant means in future network communications. MANET field is one of the most vibrant and active research fields in wireless communications networking. MANET enables the connection of devices anywhere, anyhow and anytime. MANET can be built around any wireless technology. Recently, wireless communication networks have witnessed the introductory of UWB technology. UWB transmission technique is supposed to be a promising candidate for MANET in indoor applications with short range scenarios because of its high capacity and immunity against interference.

One of the essential aspects of MANET is the development of routing protocols. In MANETs, routing protocols are needed to establish and maintain connections between nodes. Designing routing protocols in MANET depends highly on the network scenario under consideration. Therefore, routing is a very important research topic nowadays since many issues remain to be addressed. This thesis has identified key routing problems and proposed solutions to design new routing protocol for UWB MANET in an industrial indoor application, i.e., production line in a factory.

This chapter summarizes the challenges encountered in the thesis, highlights the main findings, draws conclusions and gives directions for future work.

7.1 Challenges and Solutions

UWB technology is still in the research and standardization phase during the time of performing this thesis. Moreover, prototypes of UWB transceivers are very expensive. Therefore, building a real network in an industrial environment was beyond our capabilities. The alternative solution was to define and simulate our network scenario in a well known network simulator and use this simulation code as basis for our investigations.

Simulation reliability is an important subject that has been discussed in the research community. Some researchers do not trust simulation evaluations. From our experience, we believe that simulation can be as useful as real test-beds. An important point to be noticed here is that the simulators parameters have to be set realistically. This ensures that simulation results represent the behaviors of real life systems very closely. Furthermore, a mathematical model for the channel capacity was developed as a tool for benchmarking and validation of simulation results.

Channel capacity is an important parameter in the evaluation and design of ad hoc networks. Analytical computation of channel capacity of ad hoc networks is a challenging task since it depends on many factors such as channel model, network topology, medium access, routing mechanism and traffic pattern. Therefore, some assumptions should be made to simplify mathematical derivation. Good assumptions may lead to results that can be generalized. In this thesis, we presented a simple systematic model by which the factors affecting channel capacity can be easily controlled to understand their role in channel capacity computations.

7.2 Conclusions and Main Findings

In this thesis, we defined a network scenario as basis for our investigations of routing protocols. The network scenario represents an industrial indoor application that uses UWB technology. We considered IR-UWB in this thesis. IR-UWB is based on sending very short duration pulse that can be represented by the second derivative of the Gaussian pulse. PPM and TH techniques can be used with IR-UWB to construct a multiple access communication system. TH-IR-UWB system has a large processing gain that comes from the frame repetition and the low duty cycle of the pulse. The shadowing model can be used to reflect a realistic UWB pathloss model in the PHY layer for indoor applications.

A viable industrial indoor application is a production line in a factory. UWB technology is suitable for indoor applications with a noisy environment because of its robust performance under multipath (or fading) conditions and low transmission power. Moreover, UWB technology has a very large processing gain when compared to the traditional spread spectrum systems such as WLAN. Large processing gain accompanied with large channel capacity makes UWB technology a good choice for industrial indoor applications.

A key aspect to be taken into account is the large channel capacity of UWB technology. Therefore, routing overhead can be acceptable to a certain extent in UWB ad hoc networks. However, delay in establishing routes could prevent nodes from utilizing this large capacity. Such considerations lead us to think of a routing protocol that makes use of the large capacity of UWB technology to enhance routing performance. That is, we should develop routing mechanisms that will reduce time of route establishment even if this will increase routing overhead to a certain extent. Therefore, a study on the modifications and adaptations required to adopt such a protocol in a UWB MANET was needed.

We simulated our network scenario (a production line in a factory) using ns-2 to carry out investigations on routing protocols in order to specify the basic requirements needed to design a suitable routing protocol for this scenario. MANET is trying to standardize two routing protocols: DYMO as a reactive protocol and OLSRv2 as a proactive protocol. However, we did not use these two routing protocols in our study since they are immature in terms of implementations. Moreover, they are basically developed from AODV, DSR and OLSR, and they differ mainly in packet header format. Therefore, we considered AODV, DSR and OLSR protocols in our investigations.

Although AODV and DSR are both on-demand ad hoc routing protocols, they differ in their routing mechanisms. AODV uses routing tables, one route per destination, time threshold to delete inactive routes, and destination sequence number to prevent loops and to determine the freshness of a route. On the other hand, DSR uses source routing and cache routes that maintain multiple routes per destination. DSR does not have lifetimes for route cache entries. Once a route is placed in the route cache, it can remain there until it breaks. On the other hand, OLSR is a proactive routing protocol that is optimized by limiting the number of forwarding nodes and centralizing some tasks in the network. This is done for two reasons: to reduce routing overhead using MPR node concept by which the information about the 2-hops neighborhood is flooded only; and to increase reactivity to topological changes.

The differences in routing mechanism of AODV, DSR, and OLSR lead to different performance results. We found that AODV outperforms DSR in our network scenario. In addition, AODV outperforms OLSR in small networks with low data rates (less than almost 1Kb/s). When data rate increases (greater than 1Kb/s) without increasing the network size, OLSR outperforms AODV. However, the performance of OLSR degrades as network size increases and AODV again outperforms it. Based on these results, two approaches were proposed to design efficient routing protocol for our network scenario.

Regardless the used routing protocol, the maximum values of PDR and NTh or the minimum value of ROR are achieved when the distance between mobile nodes equals to the transmission range of the nodes. This is because at this distance, number of mobile nodes in the network is optimal for multi-hop communications. If the distance between mobile nodes is smaller than the transmission range, there will be extra nodes than what are needed for multi-hop communications. On the other hand, if the distance between mobile nodes is larger than the transmission range, there will be insufficient nodes for multi-hop communications. Therefore, to get a full utilization of the production line network, the distance between mobile nodes should be adjusted to the transmission range of the nodes.

As a tool for benchmarking and validation, closed-form formulas were found for the channel capacity of ad hoc networks with line topology based on UWB and WLAN technologies. The starting point for the computation is the Shannon channel capacity equation. However, an additional restriction on channel capacity is imposed by the multiple access scheme used in the network. Furthermore, the used multiple access scheme and spread-spectrum technique affect the calculation of interference level.

It was found that the channel capacity of ad hoc networks with line topology based on WLAN technology is much lower than that based on UWB technology for the same scenario especially for a high density of nodes. This is due to the fact that the channel inside a certain coverage area in WLAN is shared by many nodes and only one node among them can access the channel at a time. In contrast, with UWB technology the channel can be accessed by all nodes simultaneously. In addition, UWB technology has a much larger processing gain. As a result, the output throughput per node is limited mainly by the transmission bit rate in case of UWB technology. On the other hand, the output throughput per node is limited mainly by a relatively low channel capacity in case of WLAN technology.

Two approaches were proposed to design efficient routing protocols for our network scenario. The first approach is based on an enhanced (or modified) protocol since AODV, DSR and OLSR have some routing mechanisms that will lead to better routing performance if they are combined in one routing protocol. The second approach is based on a new protocol with a proactive routing mechanism. Using this protocol in our scenario, nodes can exploit the information sent between fixed nodes to maintain and update routing tables automatically without the use of extra routing control packets.

We chose to focus on the first approach. As a result, we designed a new routing protocol suitable to our network scenario, and we called it Ad-Hoc On-Demand Multipath Source Routing (AOMSR) protocol. The idea was to combine many useful routing mechanisms from different routing protocols in one robust routing protocol. Therefore, by combining source routing with multiple routes per destination (DSR mechanisms) with a time threshold to

delete old routes (AODV mechanism), the problem of stale routes (drawback of DSR) is solved and the need to use frequent route discovery process (drawback of AODV) is reduced. Also, by controlling some routing tasks such as message flooding (OLSR mechanism), data packet duplication (AODV and DSR drawback) is eliminated.

AOMSR was designed in a simple and robust way. It uses routing tables, multiple route paths per destination, time threshold to delete inactive routes, and destination sequence number to determine the freshness of a route. In addition, it uses source routing mechanism to determine free-loop and disjoint paths in a robust simple way. Furthermore, AOMSR makes use of disjoint paths to control number of forwarding nodes in the network and to establish reliable route paths.

We found that AOMSR outperforms the other routing protocols considered in this study. Although it may increase routing overhead when compared to AODV, but it still achieves better throughput. Moreover, AOMSR prevents data packet duplications. The main feature that makes AOMSR suitable to our network scenario is that it reduces time of route establishment even if this may increase routing overhead to a certain extent.

7.3 Future Work

Our network scenario represents a production line in a factory. In this thesis, line topology is used since it is the common topology used in factories nowadays. This topology is suitable for large mass production of the same identical products. However, future factories try to develop production lines that are able to produce different products with small quantities. In such scenario, mesh topology could be more appropriate. In mesh topology, material boxes of different products can enter the production line from several ports along the line and also can exit from several ports. Therefore, mesh topology can be considered in future work.

Also, along the production line, material boxes are distributed uniformly in this study. Uniform distribution may not be the most realistic choice but we use it for illustrative purposes in order to establish a rough basic understanding of such network scenario. Therefore, random distribution of mobile nodes can be considered in future work.

In this thesis, we proposed two approaches to design efficient routing protocol for our network scenario. We designed AOMSR based on the first approach. Another routing protocol could be designed based on the second approach based on a proactive routing mechanism. This approach needs that the routing protocol will have two phases: transient phase and steady-state phase. In the transient phase, OLSR is used at the start up of the network to build initial routing tables since it is a proactive protocol. Then in the steady-state phase a new protocol that reduces routing overhead should be used. In our scenario, every fixed node is sending information about the moving nodes to the next fixed node regularly. Therefore, in the steady-state phase, nodes can exploit this information to maintain and update routing tables automatically without the use of extra routing control packets, since the speed and location of mobile nodes can be easily determined in this scenario. As a result, routing overhead for large network size will be decreased while maintaining fast route establishment in the same time. This could be one direction for further work.

Our model for the channel capacity is derived for the line topology configuration since it is the topology used in the production line scenario. However, following a similar systematic

procedure, our channel capacity can be modified to cope with other topology configurations as well. In other words, our model can be evolved to support research in other network scenarios. Another thing to consider for future work in our channel capacity model is that we used the pathloss power law model for radio propagation. We recommend as a future work to consider a more realistic pathloss model such as a pathloss shadowing model.

Finally, during this work, we developed ns-2 simulation codes to study routing protocols in UWB MANET deployed in an indoor industrial application. Also we developed MATLAB codes for analyzing the trace files resulting from ns-2 simulation. These codes could be useful for other users involved in the evaluation and design of ad hoc routing protocols and UWB technology.

REFERENCES

[1] Abramowitz, M. and I. R. Stegun: *Handbook of Mathematical Functions*, Dover Publications, 1970.

[2] Altman, E. and T. Jimenez: "NS Simulator for beginners," *Lecture notes 2003-2004*, Online: http://www-sop.inria.fr/maestro/personnel/Eitan.Altman/COURS-NS/n3.pdf, last access: 21/02/2008.

[3] Arslan, H. ; Z. N. Chen and M.-G. D. Benedetto (Ed.): *Ultra Wideband Wireless Communication*, John Wiley & Sons, 2006.

[4] Bali, S. and K. Jobmann: "Routing Protocols for Ultra-Wideband Mobile Ad-Hoc Networks," *IEEE Sarnoff Symposium 2008 (student paper / poster session proceeding)*, April 30, 2008.

[5] Bali, S.; J. Steuer and K. Jobmann: "Capacity of Ad Hoc Networks with Line Topology Based on UWB and WLAN Technologies," *Wireless Telecommunications Symposium (WTS)*, April 24 - 26, 2008.

[6] Bali, S.; J. Steuer and K. Jobmann: "Performance of Three Routing Protocols in UWB Ad Hoc Network Deployed in an Industrial Application," *GLOBECOM'07: IEEE Workshop on Wireless Mesh and Sensor Networks*, 30 Nov, 2007.

[7] Barrett, T. W.: "History of Ultra wideband Communications and Radar: Part 1, UWB Communications," *Microwave Journal*, pp. 22-56, January 2001.

[8] Barrett, T. W.: "History of Ultra wideband (UWB) Radar and Communications: Pioneers and Innovators," *Progress in Electronics Symposium (PIERS) 2000*, Cambridge MA, July 2000.

[9] Benedetto, M.-G. D.; L. D. Nardis; G. Giancola; S. Héthuin; I. Bucaille and F. Legrand: "Description of ad-hoc networks scenarios and potential routing algorithms," *IST – 2001-32710 U.C.A.N.*, D41-2, 2003.

[10] Brosch, J.; D. A. Maltz; D. Johnson; Y.-C. Hu and J. Jetcheva: "A Performance Comparison of Multi-Hop Wireless Ad Hoc Network Routing Protocols," *International Conference on Mobile Computing and Networking (MobiCom) 1998*, pp. 85-97, 1998.

[11] Cassioli, D.; M. Z. Win and A. F. Molisch: " The Ultra-Wide Bandwidth Indoor Channel: From Statistical Model to Simulations," *IEEE Journal on Selected Areas in Communications*, vol. 20, no. 6, pp. 1247-1257, August 2002.

[12] Chakeres, I. and C. Perkins: "Dynamic MANET On-demand (DYMO) Routing," *Internet draft, draft-ietf-manet-dymo-12.txt*, February 2008.

[13] Clausen, T.; C. Dearlove and P. Jacquet: "The Optimized Link State Routing Protocol version 2," *Internet draft, draft-ietf-manet-olsrv2-04.txt*, July 2007.

[14] Clausen, T.; P. Jacquet; A. Laouiti; P. Muhlethaler; A. Qayyum and L. Viennot: "Optimized Link State Routing Protocol," *IEEE INMIC 2001*, Lahore, Pakistan, December, 2001.

[15] Cramer, R. J.-M.; R. A. Scholtz and M. Z. Win: "On the analysis of UWB Communication Channels," *IEEE MILCOM*, vol. 2, pp. 1191-1195, Atlantic City, NJ, November 1999.

[16] Cramer, R. J.-M.; R. A. Scholtz and M. Z. Win: "The evaluation of an Ultra-Wideband Propagation Channel," *IEEE Transactions on Antennas and Propagation*, vol. 50, no. 5, pp. 561-570, May 2002.

[17] Das, S. R.; C. E. Perkins and E. M. Royer: "Performance Comparison of Two On-demand Routing Protocols for Ad Hoc Networks," *IEEE INFOCOM 2000*, pp. 3-12, 2000.

[18] Edwards, C.H. and D. E. Penney: *Calculus with Analytic Geometry*, Prentice-Hall, 1994.

[19] Federal Communications Commission: "Revision of Part 15 of the Commission's Rules Regarding Ultra-Wideband Transmission Systems," *First Report and Order,* FCC 02-48, pp. 98-153, April 22, 2002.

[20] Fontana, R. J.: "Recent System Applications of Short-Pulse Ultra-Wideband (UWB) Technology," *IEEE Transactions on Microwave Theory and Techniques*, vol.52, no.9, pp.2087–2104, Sept. 2004.

[21] Ghassemzadeh, S. S.; R. Jana; C. Rice; W. Turin and V. Tarokh: "Measurement and Modeling of an Ultra-Wide Bandwidth Indoor Channel," *IEEE Transactions on Communications*, vol. 52, No. 10, pp. 1786–1796, October 2004.

[22] Ghassemzadeh, S. S. and V. Tarokh: "UWB path loss characterization in residential environments," IEEE *Radio Frequency Integrated Circuits (RFIC) Symposium*, June 2003.

[23] Gupta, P. and P. R. Kumar: "The Capacity of Wireless Networks," *IEEE Transactions on Information Theory*, vol. 46, no. 2, pp. 388-404, 2000.

[24] Hekmat, R.: *Ad-hoc Networks: Fundamental Properties and Network Topologies*, Springer, 2006.

[25] Hekmat, R. and P. V. Mieghem: "Interference in Wireless Multi-hop Ad-hoc Networks and its Effect on Network Capacity," *Wireless Networks Journal*, vol. 10, No. 4, pp. 389-399, 2004.

[26] IEEE 802.15 WPAN Low Rate Alternative PHY Task Group 4a (TG4a), Online: http://www.ieee802.org/15/pub/TG4a.html, last access: 31/01/2008.

[27] Johnson, D. B.; D. A. Maltz and J. Broch: "DSR: the Dynamic Source Routing Protocol for Multihop Wireless Ad Hoc Networks," *Ad Hoc Networking*, C. E. Pekins (Ed.), pp. 139-172, Addison-Wesley, 2001.

[28] Johansson, P.; T. Larsson; N. Hedman; B. Mielczarek and M. Degermark: "Scenario-based Performance Analysis of Routing Protocols for Mobile Ad-hoc Networks," *International Conference on Mobile Computing and Networking (MobiCom) 1999*, pp. 195-206, 1999.

[29] Li, J.; C. Blake; D. De Couto; H. Lee and R. Morris: "Capacity of Ad Hoc Wireless Networks," *Proceedings of the 7th ACM International Conference MobiCom '01*, pp. 61-69, July 2001.

[30] Linux homepage, Online: http://www.linux.org/, last access: 21/02/2008.

[31] Malkin, G. S. and M. E. Steenstrup: "Distance-Vector Routing," *Routing in Communications Networks*, M. Steenstrup (Ed.), pp. 83-98, Prentice-Hall, 1995.

[32] MANET Working Group, Online: http://www.ietf.org/html.charters/manet-charter.html/, last access: 11/02/2008.

[33] Marina, M. K. and S. R. Das: "Ad Hoc On-Demand Multipath Distance Vector Routing," *Wireless Communications and Mobile Computing*, Vol. 6, Issue 7, pp. 969-988, 2006.

[34] MATLAB software, Online: http://www.mathworks.com/, last access: 19/02/2008.

[35] Meeneghan, P. and D. Delaney: "An Introduction to NS, Nam and OTcl scripting," *Technical Report Series: NUIM-CS-TR-2004-05*, Online: http://www.cs.nuim.ie/research/reports/2004/nuim-cs-tr-2004-05.pdf, last access 21/02/2008.

[36] Merz, R.; J.-Y. L. Boudec and J. Widmer: "An Architecture for Wireless Simulation in NS-2 Applied to Impulse-Radio Ultra-Wide Band Networks," *10th Communications and Networking Simulation Symposium (CNS'07)*, 2007.

[37] Merz, R.; J. Widmer; J.-Y. L. Boudec and B. Radunovic: "A Joint PHY/MAC Architecture for Low-Radiated Power TH-UWB Wireless Ad-Hoc Networks," *Wireless*

Communications and Mobile Computing Journal, Special Issue on UWB Communications, Vol. 5, Nr. 5, pp. 567-580, 2005.

[38] Microsoft homepage, Online: http://www.micosoft.com/, last access: 21/02/2008.

[39] Molisch, A. F.; K. Balakrishnan; D. Cassioli; C.-C. Chong; S. Emami; A. Fort; J. Karedal; J. Kunisch; H. Schantz; U. Schuster and K. Siwiak: "IEEE 802.15.4a channel model – final report," Online: http://www.ieee802.org/15/pub/2004/15-04-0662-02-004a-channel-model-final-report-r1.pdf, last access: 19/02/2008.

[40] Molisch, A. F.; J. R. Foerster and M. Pendergrass: "The Evaluation of Wireless LANs and PANs-Channel Models for Ultra wideband Personal Area Networks," *IEEE Transaction on Wireless Communications*, vol. 10, no. 6, pp. 14-21, December 2003.

[41] Moy, J.: "Link-State Routing: " *Routing in Communications Networks*, M. Steenstrup (Ed.), pp. 135-157, Prentice-Hall, 1995.

[42] Mulloy, R.: "MSSI Successfully Installs FCC Certified Ultra Wideband (UWB) Asset Tracking System for Aircraft Engine Location and Identification," *MSSI Press Release*, Germantown, MD, September 2003.

[43] Nasipuri, A; R. Castaneda and S. R. Das: "Performance of multipath routing for on-demand protocols in mobile ad hoc networks," *ACM/Kluwer Mobile Networks and Applications (MONET)*, Vol. 6, Nr. 4, pp. 339–349, 2001.

[44] Negi, R. and A. Rajeswaran: "Capacity of Power Constrained Ad-hoc Networks," *IEEE INFOCOM 2004*, pp. 443-453, 2004.

[45] Network Simulator (ns-2), Online: http://www.isi.edu/nsnam/ns/, last access: 18/02/2008.

[46] Network Simulator Manual, Online: http://www.isi.edu/nsnam/ns/doc/ns_doc.pdf, last access: 21/02/2008.

[47] Oppermann, I.; M. Haemaelaeinen and J. Iinatti: *UWB Theory and Applications*, John Wiley and Sons, 2004.

[48] Perkins, C. E. and E. M. Royer: "The Ad Hoc On-Demand Distance Vector Protocol," *Ad Hoc Networking*, C. E. Pekins (Ed.), pp. 173-219, Addison-Wesley, 2001.

[49] Pozrikidis, C.: *Introduction to C++ programming and graphics*, Springer, 2007.

[50] Prasad, R.: *Universal Wireless Personal Communications*, Artech House Publishers, 1998.

[51] PULSERS - Pervasive Ultra-wideband Low Spectral Energy Radio Systems, Online: http://www.pulsers.eu/, last access: 31/01/2008.

[52] Ross, G. F.: "Transmission and Reception System for Generating and Receiving Base-Band Duration Pulse Signals without Distortion for Short Base-Band Pulse Communication Systems," *U.S. Patent 3,728,632*, issued April 17, 1973.

[53] Scholtz, R. A.: "Multiple Access with Time-Hopping Impulse Modulation," *IEEE MILCOM*, vol. 2, pp. 447-450, Boston, MA, October 1993.

[54] Scholtz, R. A.; R. J.-M. Cramer and M. Z. Win: "Evaluation of the Propagation Characteristics of Ultra-Wideband Communication Channels," *IEEE International Antennas and Propagation Society Symposium*, vol. 2, pp. 626-630, Atlanta, GA, June 1998.

[55] Shannon, C. E.: "A Mathematical Theory of Communications," *Bell System Technical Journal*, vol. 27, pp. 379-423 and 623-656, July and October, 1948.

[56] Simulation Software, Online: http://www.ikt.uni-hannover.de/index.php?id=publikationen0, last access: 18/02/2008.

[57] Siwiak, K. and D. McKeown: *Ultra-Wideband Radio Technology*, John Wiley & Sons, 2004.

[58] Smithson, M.: *Confidence Intervals*, Series: Quantitative Applications in the Social Sciences, Sage Publications, Inc, 2003.

[59] Supplement to IEEE Standard 802.11-1999: "Part-11: Wireless LAN Medium Access Control (MAC) and Physical Layer (PHY) Specification: High-speed Physical Layer in 5 GHz Band," *IEEE standard 802.11a*, 1999.

[60] Time Domain Corporation: *Comments of Time Domain Corporation*, Docket 98-154, 1998.

[61] UCAN - Ultra wideband Concepts for Ad-hoc Networks, Online: http://www.prorec-projekte.de/ucan/, last access: 31/01/2008.

[62] UM-OLSR software, Online: http://masimum.dif.um.es/?Software:UM-OLSR, last access: 19/02/2008.

[63] UWB research at EPFL-IC, Online: http://icawww1.epfl.ch/uwb/, last access: 19/02/2008.

[64] Wikipedia – the free encyclopedia, Online: http://en.wikipedia.org/wiki/Production_line, last access: 18/02/2008.

[65] Win, M. Z. and R. A. Scholtz: "Ultra-Wide Bandwidth Time-Hopping Spread-Spectrum Impulse Radio for Wireless Multiple-Access Communication," *IEEE Transaction On Communications*, vol. 48, pp. 679–690. 2000.

WISSENSCHAFTLICHER WERDEGANG

Persönliche Daten

Name:	Samer Bali
Geburtsdatum:	03.Juni 1976
Geburtsort:	Jericho
Familienstand / Kinder:	Verheiratet / 2
Nationalität:	Palästinenser

Studienvorbereitung

09.1991 – 07.1994   Gymnasium (Jerusalem, Palästina)
Note: 96.5%

Studium

10.1994 – 09.1998   Studium zum **B.Sc. in Elektronik**
Al-Quds Universität (Jerusalem, Palästina)
Note: 92.5%

10.1999 – 09.2001   Studium zum **M.Sc. in Elektrotechnik / Kommunikation**
Universität Jordanien (Amman, Jordanien)
Note: 90.5%

Berufstätigkeit

09.1998 – 09.1999   Wissenschaftliche Hilfskraft
Fakultät für Ingenieurwissenschaften / Elektronik Abteilung
Al-Quds Universität (Jerusalem, Palästina)

04.2003 – 09.2004   Dozent
Fakultät für Ingenieurwissenschaften / Elektronik Abteilung
Al-Quds Universität (Jerusalem, Palästina)

seit 04.2005   Wissenschaftlicher Mitarbeiter
Institut für Kommunikationstechnik
Leibniz Universität Hannover